Sustainable Advances in SLA/DLP 3D Printing Materials and Processes

Erin M. Maines[a†], Mayuri K. Porwal[a†], Christopher J. Ellison[a]*, Theresa M. Reineke[b]*

[a] Department of Chemical Engineering and Materials Science, University of Minnesota, Minneapolis, Minnesota 55455, United States

[b] Department of Chemistry, University of Minnesota, Minneapolis, Minnesota 55455, United States

[†]Co-first authors

Email: maine030@umn.edu, porwa001@umn.edu

*Corresponding authors

Email: cellison@umn.edu, treineke@umn.edu

TOC Graphic

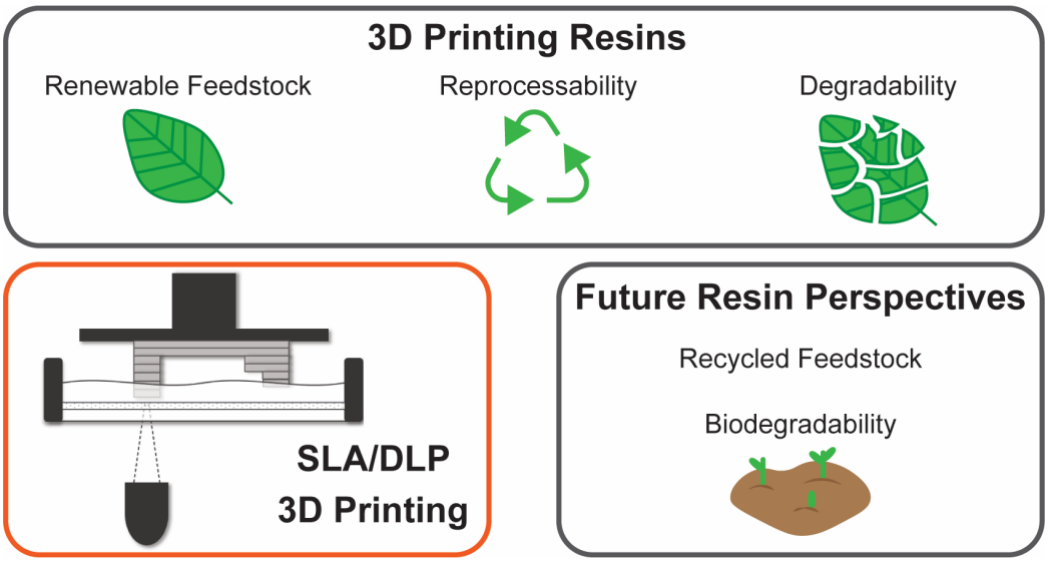

The 3D printing market is booming in various sectors coupled with an alarming increase in 3D printed plastic waste. This review summarizes sustainable advances in SLA/DLP plastic 3D printing to date and offers a perspective for further developments.

Abstract

3D printing is an essential tool for rapid prototyping in a variety of sectors such as automotive and public health. The 3D printing market is booming, and it is projected that it will continue to thrive in the coming years. Unfortunately, this rapid growth has led to an alarming increase in the amount of 3D printed plastic waste. 3D printing processes such as stereolithography (SLA) and digital light projection (DLP) in particular generally produce petroleum-based thermosets that are further worsening the plastic pollution problem. To mitigate this 3D printed plastic waste, sustainable alternatives to current 3D printing materials must be developed. The present review provides a comprehensive overview of the sustainable advances in SLA/DLP 3D printing to date and offers a perspective on future directions to improve sustainability in this field. The entire life cycle of 3D printed parts has been assessed by considering the feedstock selection and the end-of-use of the material. The feedstock selection section details how renewable feedstocks (from lignocellulosic biomass, oils, and animal products) or waste feedstocks (e.g., waste cooking oil) have been used to develop SLA/DLP resins. The end-of-use section describes how materials can be reprocessed (e.g. thermoplastic materials or covalent adaptable networks) or degraded (through enzymatic or acid/base hydrolysis of sensitive linkages) after end-of-use. In addition, studies that have employed green chemistry principles in their resin synthesis and/or have shown their sustainable 3D printed parts to have mechanical properties comparable to commercial materials have been highlighted. This review also investigates how aspects of sustainability, such as recycling for feedstock/end-of-use or biodegradation of 3D printed parts in natural environments can be incorporated as future research directions in SLA/DLP.

Introduction

The field of additive manufacturing, also known as 3D printing, has emerged as an important tool for rapid prototyping and scaled manufacturing applications in the automotive, aerospace, and public health sectors.[1–4] The 3D printing market has experienced an annual growth rate of over 10% in the past few years, and this trend is expected to continue.[2,3] While this rapid growth rate encompasses different types of additive manufacturing, this review will focus primarily on the additive manufacturing of plastic materials. An increase in the creation and therefore disposal of these plastics produced from the additive manufacturing process will further aggravate the worsening plastic pollution problem the world is already facing. Alarmingly, from 1950 to 2017, 6300 million metric tonnes of plastic waste have been discarded in landfills or the natural environment.[5] Hence, mitigating production and accumulation of plastic waste is a crucial step for the 3D printing industry, and it can be achieved by making 3D printable plastics more sustainable.

One plastic 3D printing method, Fused Deposition Modeling (FDM), already incorporates multiple aspects of sustainability in its material design, which prevents these 3D printed products from being immediately landfilled after use. FDM creates thermoplastic parts that can be reprocessed and reused which prevents waste. Additionally, one class of commercially available FDM filament is made from polylactide, which is a biobased (derived from corn starch)[6] and biodegradable material allowing for both a renewable feedstock and end-of-life composting method.

In this review, we highlight and evaluate the sustainability status of plastic materials made through the process of vat polymerization, more commonly known as stereolithography (SLA) or digital light projection (DLP). A few examples in this review will also discuss plastic materials

made via microstereo-thermal-lithography (μSTL), direct laser writing (DLW), and two-photon photopolymerization (TPP). All of these printing techniques operate via a similar process (Figure 1) with minor changes to the light source (i.e., laser versus digital light projector) and position of the light source (below, as shown in Figure 1, or above the resin tank)[7]. These methods use UV light to predominantly create chemically crosslinked polymeric materials (also known as thermosets) mostly derived from petroleum feedstocks. Unfortunately, since these materials cannot be degraded or reprocessed, they are landfilled or dumped in the environment after use, further contributing to plastic waste.

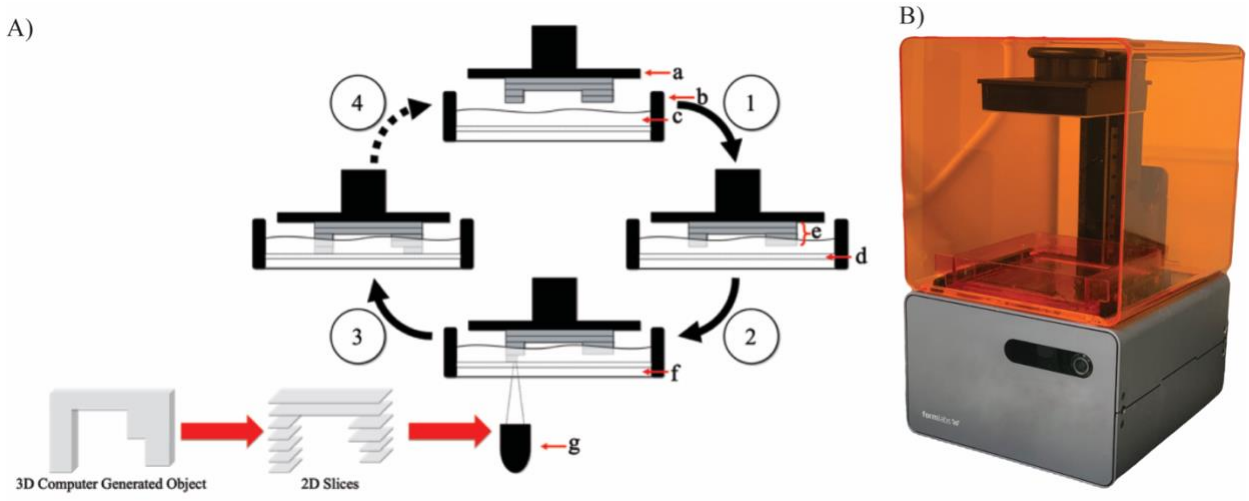

Figure 1: A) Illustration of the 3D printing process adapted from Hull C.W.[7] 1) The build plate (a) lowers into the photopolymerizable liquid resin (c), which is contained in the resin tank (b) until either the build plate (if the beginning of the printing process) or the other UV cured layers (e) are about one layer thickness away from the polydimethylsiloxane layer (d). 2) The 2D computer generated slices (which are created from the 3D computer generated object) are fed to the UV light source (g). The UV light source exposes the liquid resin to UV light through the optical window (f) to photopolymerize the resin. 3) Once the full 2D layer is completely exposed to UV light the photopolymerizable resin is adhered to the previous layer (or build plate if it is the

first layer) and the polydimethylsiloxane release layer. 4) The build plate then lifts up, peeling the last printed layer from the polydimethylsiloxane layer leaving it adhered to the build plate. This process (steps 1-4) then repeats until the full 3D part is generated. **B)** Image of a Formlabs Form 1+ Commercial 3D Printer.

A recent review article gave a good overview on sustainable photopolymers for SLA and DLP 3D printing materials.[8] The present review aims to expand on this by providing a comprehensive overview of sustainable advances in SLA/DLP, while also offering a perspective on future directions of sustainability. Herein, the entire life cycle of 3D printed materials is framed by considering the following main categories: 1. Feedstock (1.1 Renewable and 1.2 Waste) and 2. End-Of-Use (2.1 Reprocessable Materials and 2.2 Degradable Materials) as outlined in Table 1 below.[9] The feedstock selection provides an overview of how renewable feedstocks (e.g., lignocellulosic biomass, oils, and animal products) and waste feedstocks (e.g., waste cooking oil) have been utilized to develop SLA/DLP resins. Both of these feedstock selections improve the sustainability of SLA/DLP materials by eliminating the reliance on petroleum-based feedstocks. The end-of-use section focuses on materials that can be reprocessed (e.g. through creation of non-crosslinked thermoplastic materials, or through the creation of covalent adaptable networks that are crosslinked but can undergo changes when a stimulus such as heat is applied) or degraded (e.g. through enzymatic or acid/base hydrolysis of sensitive linkages such as ester linkages). Both reprocessing and degradation of 3D printed parts after end-of-use could help alleviate the problem of 3D printed plastic waste. Additionally, throughout the document and in Table 1, special attention is placed on studies that employ greener synthesis techniques, such as elimination of organic solvents during synthesis and elimination of photoinitiators from the monomer formulation. Eliminating or substituting organic solvents with benign alternatives during synthesis

is particularly important since most organic solvents are toxic, flammable, and also comprise a majority of the waste in the synthesis processes.[10,11] Furthermore, eliminating the photoinitiator reduces the number of additives necessary for the formulation making them potentially safer and more sustainable. This is significant as some commercial photoinitiators have been noted to have high toxicity. For example, a commonly employed photoinitiator such as diphenyl(2,4,6-trimethylbenzoyl)phosphine oxide (more commonly known as TPO) has been declared as toxic and hazardous by the European Chemicals Agency (ECHA).[12,13]

In addition to green synthetic methods, sustainable SLA/DLP materials with mechanical and thermal properties comparable to commercially available materials have also been highlighted. This is important as sustainable resins can be used to replace commercial petroleum-based 3D printing resins only if the properties are comparable. To evaluate mechanical properties of 3D printed parts, two characterization techniques are primarily used: tensile tests and flexural strength tests, such as the three-point bending test. Tensile testing is one of the most popular mechanical characterization techniques and can be performed in two different modes: tension (pulling on the material) or compression (pushing on the material). Material parameters that can be determined from tensile testing in either of the modes include: the Young's modulus or the compression modulus (which indicates material stiffness or resistance to deformation under tension or compression, respectively), strain/elongation at break (which indicates how much the material can be stretched or compressed before it fractures), tensile or compressive strength (which indicates the maximum stress a material can withstand before it fractures), and toughness (which measures the ability of a material to absorb energy until fracture).[14] Generally from tensile test studies material toughness can be determined by calculating the area under the stress-strain curve up to the point of fracture.[14] The Young's modulus can be determined from the slope of the stress-strain

curve in the linear elastic or Hookean regime. In general, materials with low strain at break that fracture while deforming elastically are considered brittle, whereas materials with high elongations at break that deform plastically before fracture are referred to as ductile.[14] On the other hand, flexural strength tests are performed to determine the flexural or bending modulus of materials, which indicates the tendency of material to resist bending (a low flexural modulus corresponds to high flexibility). Typical commercial 3D printed resins such as Formlabs clear resin (which is mentioned throughout this article) is relatively stiff with a Young's modulus of 2.8 GPa and a flexural modulus of 2.2 GPa.[15] Finally, thermal properties of 3D printed parts have been evaluated using differential scanning calorimetry to determine the glass transition temperature (T_g) and the melting temperature (T_m), which are critical design parameters. Materials used below their T_g are rigid solids while materials used between their T_g and T_m are soft. Interestingly, very few crystalline SLA/DLP 3D printed materials have been reported, hence most materials discussed in this review only report a T_g.

Finally, while significant progress towards more sustainable SLA/DLP materials has been made through the use of renewable feedstocks, waste feedstocks, reprocessable materials, and degradable materials, there are a few unexplored areas that will be highlighted at the end as opportunities for possible future research. These aspects include chemical recycling of 3D printed parts to recover monomers, recycling of 3D printed material for reuse in the photopolymerization process, and evaluating other methods of biodegradation in natural environments.

Table 1: Overview of research and topics covered in this review.

Renewable Feedstock

Base Feedstock	Key Polymerizable Groups	Type of 3D Printing	Additional Notable Aspects of Sustainability	Sources
Lignin	Acrylate, Methacrylate, Coumarin	SLA/DLP	Solvent free synthesis;[19-21] Elimination of harmful reagents (Photoinitiator);[24] Competitive material properties with commercial resins;[20,22] Photopolymerizable groups from renewable sources (Coumarin)[24]	19-22, 24
Cellulose	Methacrylate	SLA	Degradation (Hydrolytic)	27
Sucrose	Methacrylate, Acrylate	SLA	Solvent free synthesis; Competitive material properties with commercial resins	28
CL	Methacrylate, Acrylate	SLA/DLP	Degradation (Hydrolytic and enzymatic)[29,32,33]	29, 30, 32 - 34
LA	Methacrylate, Fumarate	SLA	Photopolymerizable groups from renewable sources (Fumaric acid, non-toxic)[36]	35, 36, 81
Terpenes	Thiol + vinyl, thiol + allyl, thiol + cyclohexene	DLP	Photopolymerizable groups from renewable sources (Terpene double bonds)	41, 42
Diacids	Methacrylate, Alkenes	DLP/μSTL	Solvent free synthesis[44]	43, 44
Linseed Oil	Epoxy	DLP/SLA	-	48, 49
Soybean Oil	Acrylate, Methacrylate	SLA/DLP/ DLW	Solvent free synthesis;[52] Competitive material properties with commercial resins[52]	50-53
Biogenic Amines	Methacrylate, Thiol + allyl	DLP	Elimination of harmful reagents (Isocyanates);[63,64] Solvent free synthesis; Bioderived light absorber (Dopamine)[66]	63, 64, 66
Silk Fibroin	Methacrylate	DLP	Replacement of harmful solvents	59
Globular Proteins	Methacrylate	SLA	Degradation (Enzymatic); Replacement of harmful solvents	68
Hyaluronic acid		DLP	-	69
Alginate	Ionic Associations	SLA	Degradation; Replacement of harmful solvents	70
Keratin		DLP	Replacement of harmful solvents and reagents (inhibitor, catalyst, and initiator)	71

Waste Feedstock

Base Feedstock	Key Polymerizable Groups	Type of 3D Printing	Additional Notable Aspects of Sustainability	Sources
Waste Cooking Oil	Acrylate	DLP	Biodegradation by soil burial; Solvent free synthesis; Recovery and reuse of monomers, catalyst, and solvent used in purification	72
Carbon Dioxide	Methacrylate	DLP	Solvent free synthesis; Elimination of harmful reagents (Isocyanates); Competitive material properties with commercial reins	73

Reprocessable Materials

Base Feedstock	Key Polymerizable Groups	Type of 3D Printing	Additional Notable Aspects of Sustainability	Sources
Hexane di-thiol and di-allyl terephthalate	Thiol + allyl	DLP	Thermoplastic	74
Acryloylmorpholine	Acryloyl	DLP	Thermoplastic	75
Bisphenol A Glycerolate di-(meth)acrylate	Acrylate	DLP/SLA	Dynamic covalent network (transesterification); Elimination of catalyst[77]	77, 76
Hydroxyethyl acrylate	Acrylate	DLP	Dynamic covalent network (Diels-Alder)	78

Degradable Feedstock

Base Feedstock	Key Polymerizable Groups	Type of 3D Printing	Additional Notable Aspects of Sustainability	Sources
Propylene oxide and maleic anhydride	Fumaric double bond	SLA	Degradation (hydrolytic); Degradation products (nontoxic)	83,84
CL and TMC	Acrylate	DLP	Renewable feedstock; Degradation (hydrolytic)	31
CL and LA	Methacrylate	TPP	Renewable feedstock; Degradation (hydrolytic)	37
Adipic Acid and triethylene glycol	Methacrylate	SLA	Renewable feedstock; Degradation (hydrolytic)	85
1,4-Butanediol, 1,1,1-Tris(hydroxy methyl)propane	Thiol + propargyl, thiol + butyne-1-yl	DLP	Degradation (hydrolytic); Degradation products (low molecular weight fragments)	86
Gelatin	Methacrylate	TPP	Renewable feedstock; Degradation (enzymatic)	87

1. Feedstock Selection

1.1 Renewable Feedstock

1.1.1 Lignocellulosic Biomass

An important source of renewable feedstock is lignocellulosic biomass due to its worldwide abundance.[16] Lignocellulosic biomass is composed of agricultural waste (e.g. sugarcane bagasse, rice straw, and wood pellets) and low-cost energy grasses such as switch grass.[17,18] The three major components of lignocellulosic biomass are lignin (10-20 wt%), hemicellulose (15-35 wt%), and cellulose (35-50 wt%).[18] With the help of various thermochemical conversion processes, lignocellulosic biomass can be converted to over 200 value-added renewable chemicals.[5] In this section, we will briefly summarize how various lignocellulosic biomass-derived renewable chemicals have been efficiently utilized in 3D printing to develop photocurable resins. For a summary of the materials and papers discussed in this section please see Table 1. For additional information on materials obtained from lignocellulosic biomass and their uses in UV curable 3D printing materials please refer to this recent review article.[19]

1.1.1.1 Biobased Phenolics and Saccharides

Biobased phenolics derived from lignin have been used to synthesize photopolymerizable SLA resins. Lignin has been used in SLA resins in several different ways, such as using acrylate functionalized bulk lignin or breaking down lignin into individual monomers to create monofunctional (meth)acrylates. When bulk lignin is functionalized with acrylates it can be incorporated into a resin as a bio-derived lignin acrylate crosslinker with many acrylate crosslinking sites. Sutton *et.al.* demonstrated that 92% of the hydroxy groups on bulk lignin can be acrylate functionalized under solvent-free conditions (Figure 2) and up to 15 wt% of this crosslinker can be incorporated in a commercial SLA resin (PR48 Clear resin from Colorado

Photopolymer Solutions).[20] Increasing the amount of lignin crosslinker in the resin from 0 to 15 wt% decreases the Young's modulus from 0.65 GPa to 0.37 GPa and increases the strain at break from 1.87% to 7.6% leading to more ductile materials.[20] The authors attribute this to the plasticizing effect of additional side chains from the lignin, which decreases the crosslinking density and chain-to-chain interactions in the network.[20]

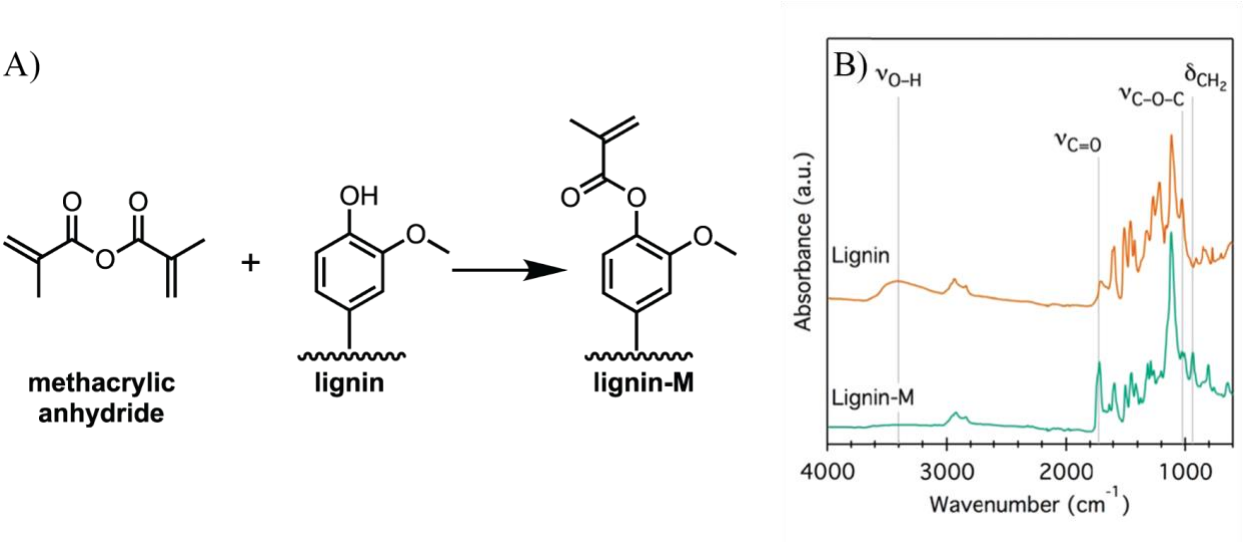

Figure 2: A) Lignin functionalization chemistry to obtain a methacrylated lignin material (lignin-M).[20] **B)** FTIR of lignin sample before functionalization (orange, top) and after functionalization (green, bottom) indicating the disappearance of the O-H peak in the bottom trace demonstrating methacrylate functionalization.[20] Reprinted with permission from {J. T. Sutton, K. Rajan, D. P. Harper and S. C. Chmely, Lignin-Containing Photoactive Resins for 3D Printing by Stereolithography, *ACS Appl. Mater. Interfaces,* 2018, **10**, 36456–36463}. Copyright {2018} American Chemical Society.

In addition to using bulk lignin, the lignin network can be broken down into bio-derived phenolic monomers (e.g. guaiacol, eugenol, and vanillin), which can be functionalized to obtain (meth)acrylates without the use of organic solvents.[21] The resulting monomers can serve as

replacements for traditional SLA materials, or they can be used to develop an entirely new renewable resin formulation. For example, Ding *et.al.* demonstrated that monofunctional guaiacol acrylate can be blended with renewable (meth)acrylates (e.g. di-functional eugenol acrylate and di-functional vanillin methacrylate) or mixed with a commercial trimethylolpropane tri-methacrylate monomer to produce SLA resins, as shown in Figure 3A.[21] These SLA resins were used to print highly intricate and detailed parts as shown in Figure 3B. In this study, a ternary mixture of guaiacol acrylate, eugenol di-acrylate, and trimethylolpropane tri-methacrylate allowed tailoring of the Young's modulus from 0.83 GPa to 1.35 GPa and the strain at break from 2.8% to 8.2% just by increasing the amount of guaiacol acrylate and reducing the amount of eugenol di-acrylate, as seen in Figure 3C.[21] In contrast, an analogous fully renewable monomer system that replaced the tri-methacrylate with vanillin di-methacrylate exhibited Young's moduli and strains at break from 1.02 GPa to 1.23 GPa and 6.9% to 8.9%, respectively (shown in Figure 3D).[21] Compared to the tensile properties of a commercial SLA resin (Formlabs clear resin; strain at break of 10.1% and tensile strength of 83.4 MPa), Figure 3D shows that the properties of these biobased phenolic materials are very similar indicating they could be suitable replacements for the Formlabs clear resin. The two discussed studies demonstrate that competitive 3D printed materials can be produced either by solely using lignin derivatives or by blending functionalized lignin with commercial supporting materials.

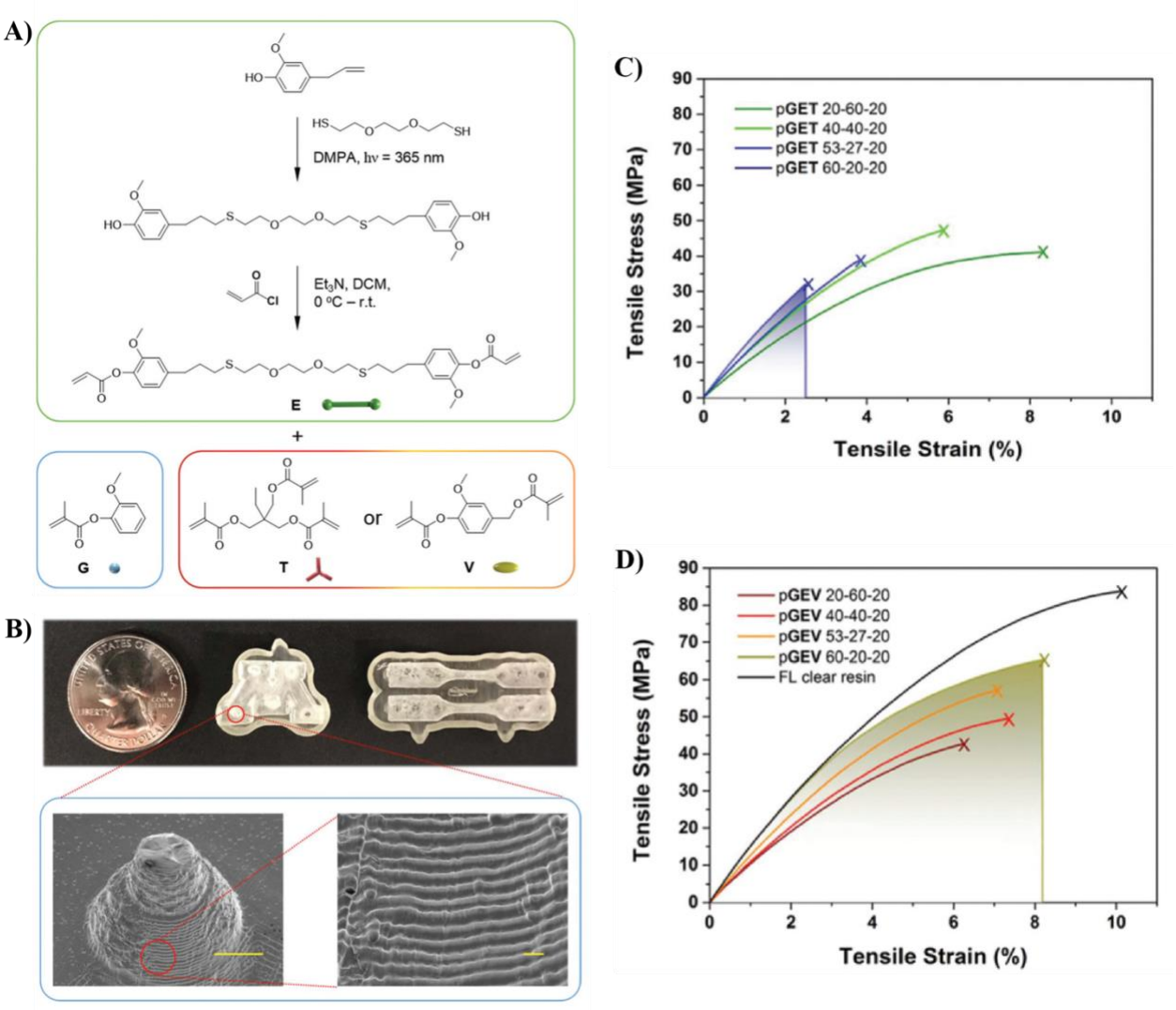

Figure 3: A) Synthesis of di-functional eugenol acrylate (E), chemical structure of guaiacol acrylate (G), vanillin di-methacrylate (V), and trimethylolpropane tri-methacrylate (T). In the synthesis of E the photoinitiator utilized is 2,2-dimethoxy-2-phenylacetophenone (DMPA).[21] **B)** Top image is a 3D printed "M" and dog-bones made from 60 mol% G, 20 mol% E, and 20 mol% V. Bottom images are SEM images of the "M" with the scale bar in the left photo being 100 mm and the scale bar in the right photo being 100 μm. **C)** and **D)** Tensile studies of networks comprising of guaiacol methacrylate (G), eugenol di-acrylate (E), and trimethylolpropane tri-methacrylate (T) (pGET) or vanillin di-methacrylate (V) (pGEV). Numbers listed after

pGEV/pGET indicate molar ratios of each respective component incorporated into the network. FL clear resin is the Formlabs commercial clear resin.[21] Reproduced from Ref. 21 with permission from the Royal Society of Chemistry.

While Ding *et.al.* used a vanillin di-methacrylate crosslinker in the resin composition, mono-methacrylated vanillin analogs have also been used to develop SLA resins.[22] Bassett *et. al.* synthesized a methacrylated vanillin monomer and glycerol di-methacrylate crosslinker via a one-pot, two-step synthetic scheme without the use of organic solvents (Figure 4).[22] Notably, a small amount of the catalyst 4-dimethylaminopyridine (DMAP) was used during synthesis (2 mol%), and other components, such as reactive diluents, were eliminated since the resin had a sufficiently low viscosity at room temperature for 3D printing.[22] Once crosslinked, these vanillin-glycerol thermosets have a very high T_g of 150 °C, high Young's modulus of 4.8 GPa, low strain at break of 0.27%, and tensile strength of 12.49 MPa.[22] Vanillin di-acrylate has also been used by Navaruckiene *et.al.* as the sole component in direct laser writing to produce thermosets with a high gel fraction of 96%.[23] In comparison to commercial materials, the vanillin di-acrylate derived materials had a much lower compression modulus (2.01 MPa) than the Formlabs clear resin (7.17 MPa), however, the compression modulus of the commercial PR48 material was much closer at 5.56 MPa.[23] Additionally, the flexural modulus of the vanillin di-acrylate mixture (9.47 MPa) was similar to the PR48 resin (8.80 MPa), but much higher than the Formlabs clear resin (1.09 MPa).[23]

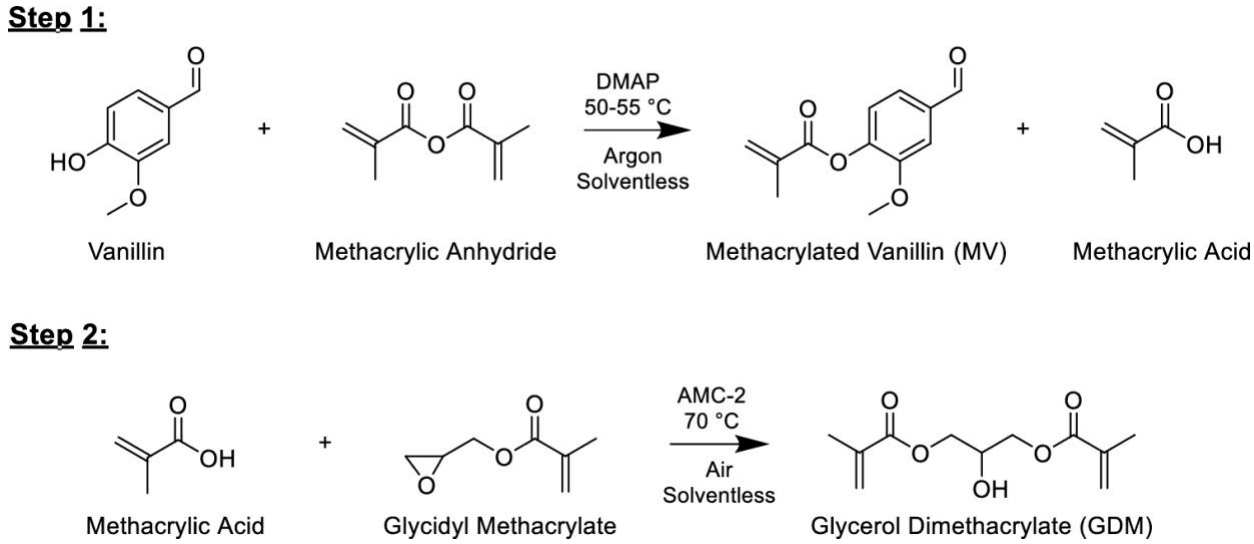

Figure 4: One-pot, two-step synthesis of methacrylated vanillin and glycerol di-methacrylate without the use of organic solvents.[22] AMC-2 is a catalyst used to prevent homopolymerization and etherification through the epoxy moiety. Reprinted with permission from {A. W. Bassett, A. E. Honnig, C. M. Breyta, I. C. Dunn, J. J. La Scala and J. F. Stanzione, Vanillin-Based Resin for Additive Manufacturing, *ACS Sustain. Chem. Eng.*, 2020, **8**, 5626–5635} Copyright {2020} American Chemical Society.

Apart from synthetic pathways directly involving phenolics from lignocellulosic biomass, other precursors, such as coumarin, can be synthesized from lignin via fermentation.[24] As an alternative to acrylates, coumarin has been explored as a photoreactive moiety in renewable resins comprising of polycaprolactone (PCL) and trimethylene carbonate (TMC), with coumarin end groups (synthesis scheme shown in Figure 5A).[25] TMC is a cyclic carbonate monomer that can be synthesized from glycerol-derived 1,3-propanediol,[26] whereas CL is a cyclic ester derived from 5-hydroxymethyl furfural (this will be described in further detail in section 1.1.1.2).[17] Eliminating acrylates changes the reaction mechanism from photopolymerization to photodimerization since coumarin dimerizes under UV light to form crosslinks. Remarkably, the use of coumarin as the photoreactive group allows for the elimination of a photoinitiator as coumarin dimerizes

spontaneously when exposed to UV light.[25] While the resulting 3D printed structures are well resolved, as shown in Figure 5B, a disadvantage of coumarin photodimerization is the significantly longer curing time (on the order of minutes) as compared to other (meth)acrylate resins with photoinitiator (on the order of seconds).[25] However, the potential benefits of eliminating a toxic photoinitiator, as outlined in the introduction, could outweigh the slightly longer exposure times. Given the majority of the material comprises of low T_g CL and TMC monomers with only minor portions of coumarin end groups, it is not surprising that the T_g was well below room temperature at −43 °C with a T_m near room temperature.[25] This study reveals that bio-derived coumarin is an interesting alternative for elimination of acrylate end groups and photoinitiators from SLA/DLP resins.

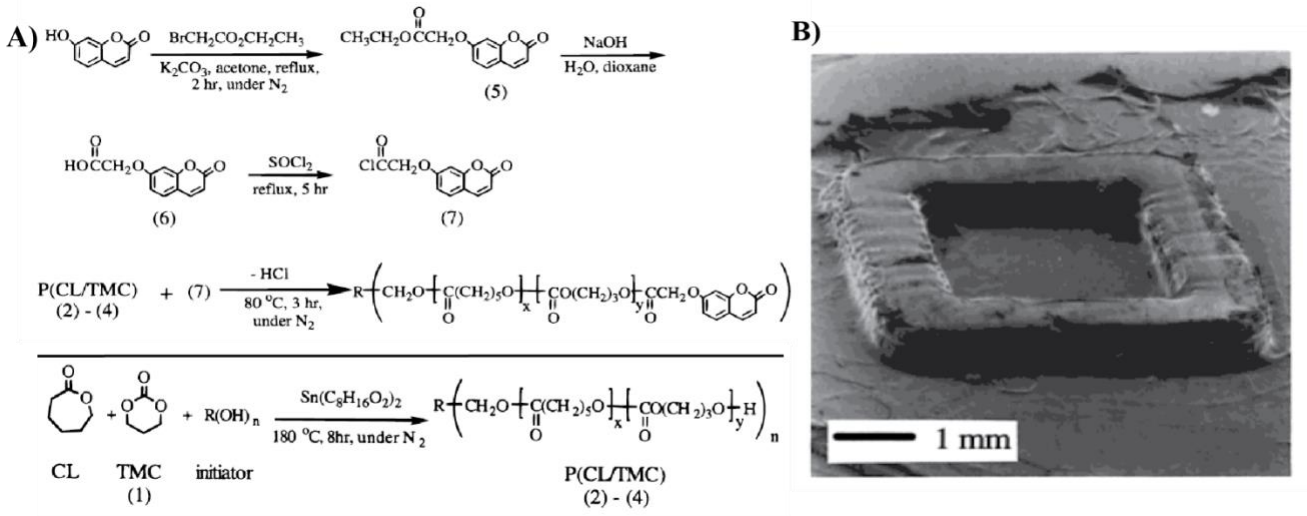

Figure 5: A) Coumarin end-group and TMC/PCL polymer synthesis.[25] **B)** SEM of the photopolymerized polymer containing coumarin end groups.[25] Reprinted with permission from {T. Matsuda, M. Mizutani and S. C. Arnold, Molecular design of photocurable liquid biodegradable copolymers. 1. Synthesis and photocuring characteristics, *Macromolecules*, 2000, 33, 795–800} Copyright {2000} American Chemical Society.

Another major component of lignocellulosic biomass, cellulose (35-50 wt%),[16,27] has also been utilized as a renewable feedstock in 3D printing formulations. Recently, Lu *et.al.* developed

a dual-cure resin from cellulose and rosin (a renewable feedstock obtained from waste wood and pine trees)[28], and 3D printed this resin via SLA to develop thermosets.[29] In this study, a two-step polymerization strategy was employed combining UV-triggered chain-growth polymerization and thermally triggered step-growth polymerization. The dual-cure resin solution comprised of methacrylated cellulose crosslinker (ECM), rosin derived methacrylate monomer (DAGMA), 2-hydroxyethyl acrylate (HEA), and hexamethylene diisocyanate (HDI) (Figure 6).[29] The formation of a dual-cure network increased the thermoset crosslink density and induced phase separation leading to thermosets with a higher T_g (51 °C) and higher rubbery plateau modulus (5.5 MPa) than one-step UV-cured thermosets (T_g of 31 °C and rubbery modulus of 3.8 MPa).[29] These results signify that the two-step polymerization strategy is beneficial in improving the thermal and mechanical properties of thermosets. The dual-cure thermoset exhibited thermally triggered shape-memory due to the combination of chemical (acrylate groups) and physical crosslinking junctions (hydrogen bonding from free hydroxyl groups of ECM and urethane-urethane/urethane-ester linkages). Interestingly, the thermosets also exhibited fluorescence due to the presence of the aromatic rings in the rosin, hydroxyl groups of ECM and HEA, and amine groups of polyurethane, since these groups enable n-π^* or π-π^* aggregation.[29] This fluorescence property is especially attractive for LED and sensor applications.

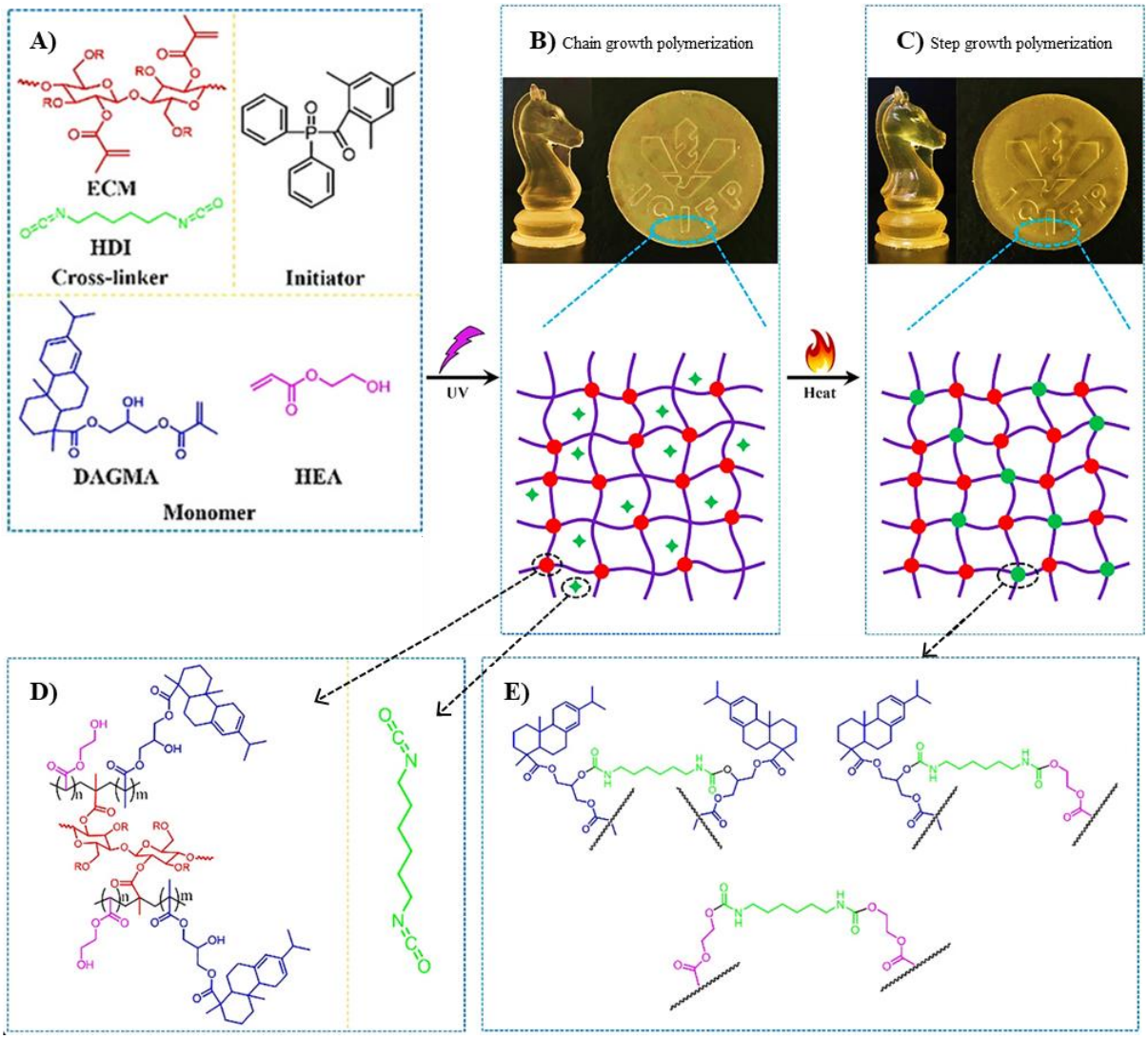

Figure 6: A) Photosensitive resin solution. **B)** Schematic representing chain growth polymerization due to ECM, HEA and DAGMA, and **C)** step growth polymerization due to HDI. Chemical structure of the resulting **D)** chain-growth and **E)** step growth networks.[29] Reprinted with permission from C. Lu, C. Wang, J. Yu, J. Wang and F. Chu, Two-Step 3 D-Printing Approach toward Sustainable, Repairable, Fluorescent Shape-Memory Thermosets Derived from Cellulose and Rosin, *ChemSusChem*, 2019, **210037**, 1–11. Copyright © 2019 Wiley-VCH Verlag GmbH & Co. KGaA, Weinheim.

The disaccharide sucrose has also been incorporated into 3D printing formulations.[30] In a recent study, epoxidized sucrose soyate (ESS) was used as a building block to synthesize three types of bio-based resins under solvent-free conditions: methacrylated butylated ESS, di-methacrylated ESS, and acrylated ESS (Figure 7A). Three different SLA formulations were developed by mixing 42 wt% of these sucrose-based resins with reactive diluents. The resulting SLA formulations were 3D printed into samples for flexural and tensile testing in different orientations (0° or 90° with respect to the build platform). The properties of 3D printed parts such as T_g, Young's modulus, and tensile strength could be widely varied over the range of 40.9 °C to 79.7 °C, 450 MPa to 1670 MPa, and 8 MPa to 17 MPa, respectively, by altering the type of sucrose-based resin, as seen below in Figure 7B.[30] The acrylated and methacrylated sucrose soyate were compared to three commercial resins: two urethane acylate resins (Ebecryl 1290 and Ebexryl 220) and Moai Blue resin.[30] As noted above, the tensile strength and Young's modulus could be tuned to be similar to the commercial resins depending on the structure of the sucrose soyate pendant groups, as shown in Figure 7B. The print orientation of the tensile bars also dramatically changed the results of the Young's modulus of di-methacrylated ESS such that it was similar to the commercial Moai Blue and greater than Ebecryl 1290 when printed in the 90° orientation, as shown in the far right graph of Figure 7B. This indicates the importance of print direction in 3D printed parts.[30]

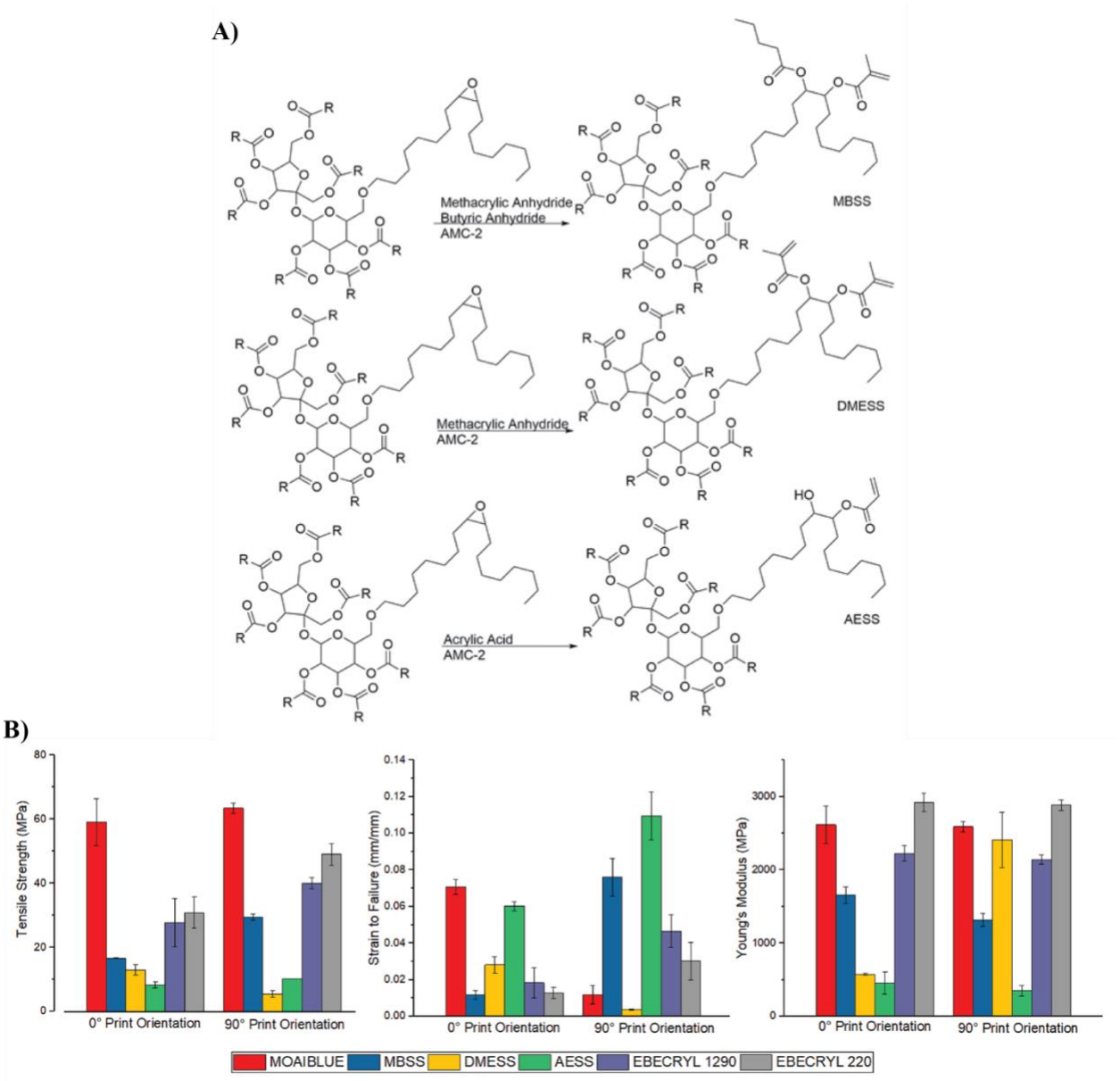

Figure 7: **A)** Synthesis of sucrose-based resins MBSS, DMESS, and AESS for SLA printing.[30] **B)** From left to right: tensile strength, tensile strain to failure, and Young's modulus.[30] Reprinted with permission from {S. D. Silbert, P. Simpson, R. Setien, M. Holthaus, J. La Scala, C. A. Ulven and D. C. Webster, Exploration of Bio-Based Functionalized Sucrose Ester Resins for Additive Manufacturing via Stereolithography, *ACS Appl. Polym. Mater*., 2020, 2, 2910–2918} Copyright {2020} American Chemical Society.

The above SLA/DLP resins satisfy many aspects of sustainability, such as being derived from renewable lignocellulosic biomass, reduction of solvent use during synthesis, and eliminating photoinitiator, while exhibiting a range of attractive properties. However, most of these examples form non-degradable or non-reprocessable linkages, such as poly(meth)acrylates. Additional work with lignocellulosic biomass derived materials could investigate incorporation of chemical linkages that impart degradability or reprocessability to address end-of-life concerns.

1.1.1.2 Polyesters

Cyclic esters such as caprolactone (CL) and lactide (LA) have been widely utilized as renewable feedstock to develop resins for 3D printing. CL and LA can be derived from 5-hydroxymethyl furfural and lactic acid, respectively, which can be readily obtained from lignocellulosic biomass as shown in Figure 8.[17]

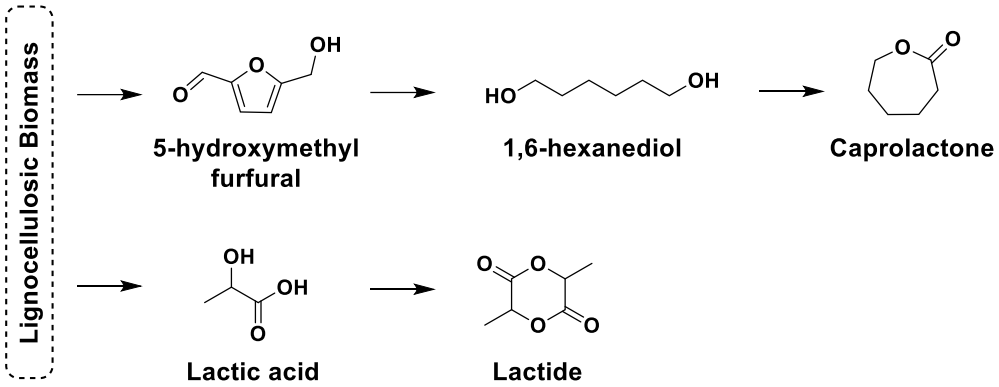

Figure 8: Conversion of lignocellulosic biomass to caprolactone and lactide.[17] Reproduced from Ref. 17 with permission from the Royal Society of Chemistry.

CL has been incorporated in 3D printing formulations alone,[31,32] as well as in combination with other cyclic ester monomers.[33–36] Elomaa *et.al.* incorporated CL by end-capping three-armed poly(caprolactone) (PCL) oligomers with methacrylate groups (Figure 9A).[31] The synthesized PCL macromers were used to print porous scaffolds via SLA without the addition of solvent. The printed scaffolds had an interconnected pore structure and high resolution as depicted in the

microcomputed tomography reconstruction and SEM images in Figure 9B.[31] The scaffolds also had a homogenous porosity in the range of 400-500 μm.[31] The high pore interconnectivity and homogeneous porosity is significant for accommodation of cells inside the scaffold and transport of nutrients when these structures are used for cell seeding and implantation.[31]

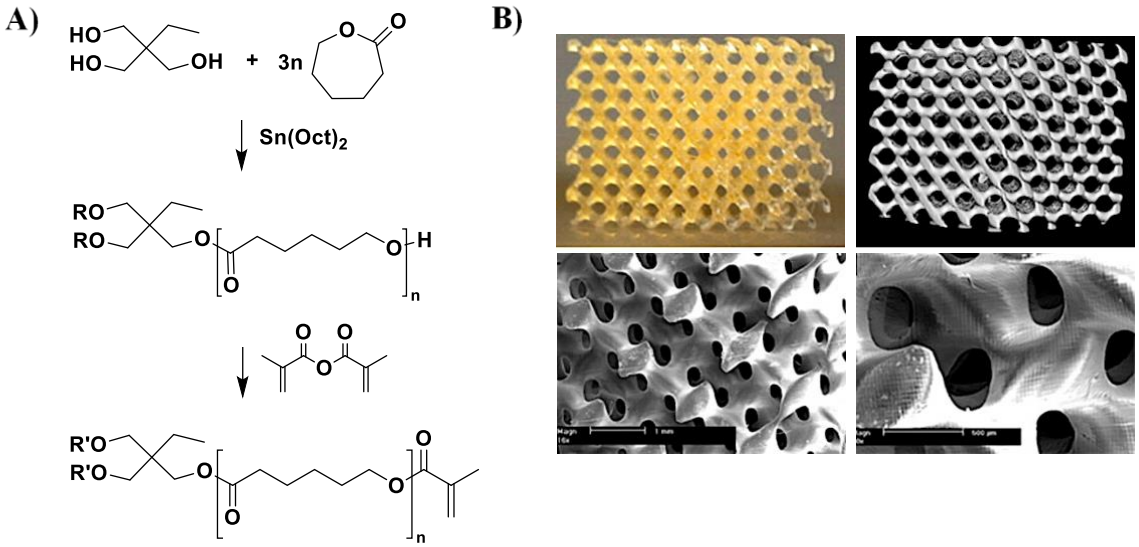

Figure 9: A) Synthesis of three-armed PCL macromers (Reproduced from Elomaa et.al.).[31] **B)** Photograph, microcomputed tomography visualization, and SEM images of SLA printed PCL scaffolds.[31] Reprinted from *Acta Biomater.*, Vol 7, L. Elomaa, S. Teixeira, R. Hakala, H. Korhonen, D. W. Grijpma, J. V. Seppälä, Preparation of poly(ε-caprolactone)-based tissue engineering scaffolds by stereolithography, 3850–3856, Copyright (2011), with permission from Elsevier.

In another study, CL was combined with a bio-based cyclic ester amide monomer to develop a new type of photocrosslinkable poly(ester-amide) resin.[34] Copolymers of CL and L-alanine based cyclic ester-amide monomer, 3-methyl-morpholine-2,5-dione (MMD), were synthesized by ring-opening polymerization (Figure 10A). These copolymers were end functionalized with methacrylate groups to produce crosslinked porous scaffolds by SLA, as shown in Figure 10B-C. Scaffolds synthesized from copolymers containing 10 mol% of MMD

had a significantly higher stiffness and compression modulus of 110 N/mm and 5.9 MPa, respectively, as compared to pure PCL based scaffolds (stiffness 60 N/mm and compression modulus 3.2 MPa).[34] This increase in compression modulus and stiffness was attributed to the strong intermolecular hydrogen bond interactions between the amide groups from the MMD units in the copolymer. Notably, this study also investigated the hydrolytic degradability of CL/L-alanine thermosets due to presence of ester linkages in the thermoset. Degradation of the films was evaluated by immersing them in phosphate buffered saline (PBS) solution at pH=7.4 at 37 °C. The thermoset degradation rate increased with MMD content. For instance, the control PCL films underwent a mass loss of 8% in 6 months, whereas films with 10 mol% MMD had a mass loss of 15% in 6 months under identical degradation conditions.[34] This faster degradation rate was attributed to the increased surface hydrophilicity of thermoset films due to MMD.[34] The thermoset films had a constant degradation rate throughout hydrolysis and maintained their shape suggesting that these films could be used in zero order drug release applications.[34]

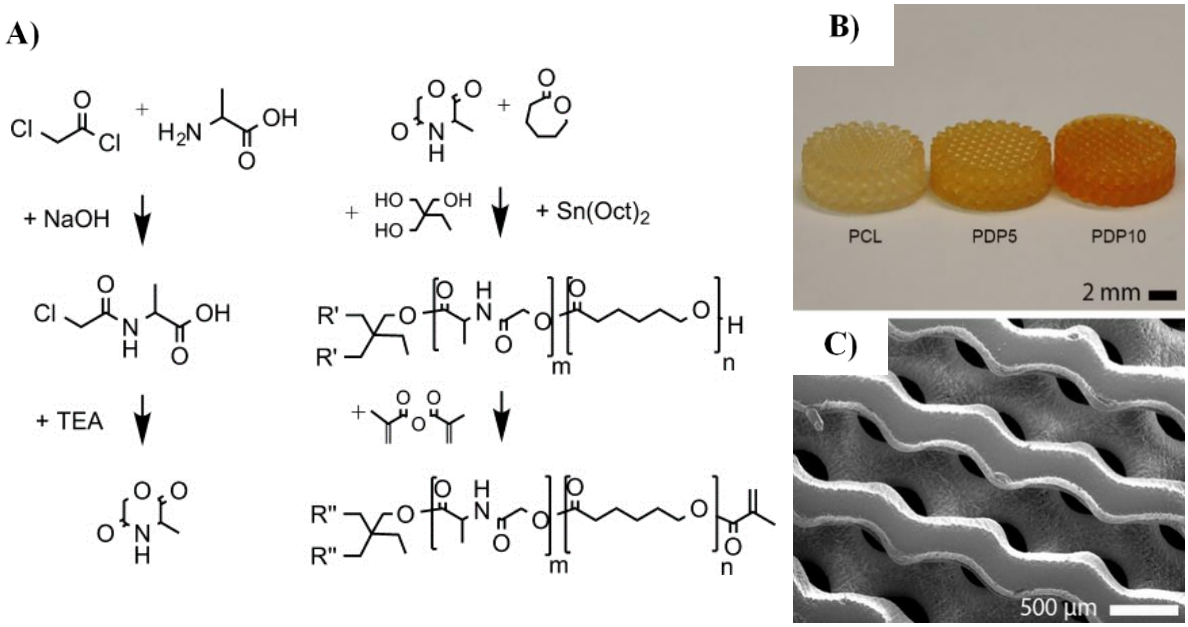

Figure 10: A) Synthesis of cyclic MMD monomer from L-alanine, and ring-opening polymerization of MMD/CL followed by methacrylation to generate photocrosslinkable

macromers (PDP).[34] **B)** Photographs of scaffolds prepared by SLA of pure PCL macromer, PDP macromers with 5 mol% (PDP5), and 10 mol% (PDP10) of MMD.[34] **C)** SEC image of the top surface of PDP10 scaffold.[34] Reprinted with permission from L. Elomaa, Y. Kang, J. V. Seppälä and Y. Yang, Biodegradable photocrosslinkable poly(depsipeptide- co -ε-caprolactone) for tissue engineering: Synthesis, characterization, and In vitro evaluation, *J. Polym. Sci. Part A Polym. Chem.*, 2014, **52**, 3307–3315. Copyright © 2014 Wiley Periodicals, Inc.

Apart from copolymerizing CL with one monomer, CL has also been incorporated in UV curable compositions containing two or more comonomers.[35,36] Chen *et.al.* developed thermosets by combining three different renewably derived polymers namely PCL, polyethylene glycol (PEG), and poly(glycerol sebacate) (PGS).[35] PEG can be synthesized by polymerization of ethylene oxide derived from bio-ethanol[17] and PGS can be obtained from polycondensation of glycerol and sebacic acid. These polymers were acrylated to synthesize photocurable polymers (Figure 11). By blending the three polymers in different ratios, the Young's modulus and elongation at break of the obtained thermosets could be tuned over a wide range of 0.12 MPa to 18.98 MPa and 121.23% to 11.28%, respectively.[35] This suggests that tissue-engineering scaffolds with varying mechanical properties could be 3D printed by blending the acrylated polymers in suitable ratios. Due to the presence of ester bonds, hydrolytic degradation of these networks was evaluated by immersing them in PBS solutions containing the enzyme lipase at 37 °C. It was found that the degradation rate was faster for networks with higher PGS content, since the PGS

backbone contains the highest number of ester linkages in the network.[35] This suggests that PGS containing thermosets could be suitable for applications as soft tissue engineering scaffolds.[35]

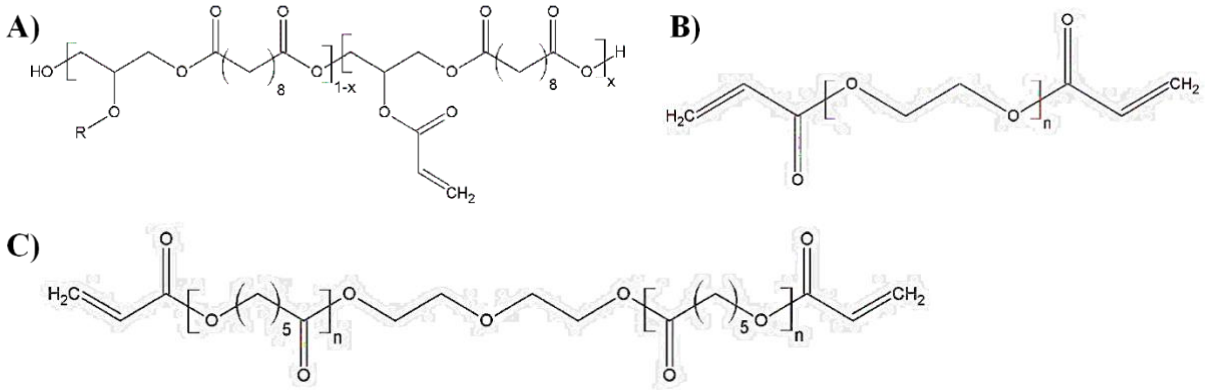

Figure 11: Chemical structures of **A)** PGS acrylate, x indicates the degree of acrylation, **B)** PEG di-acrylate, and **C)** PCL di-acrylate.[35] Reproduced from Ref. 35 under the terms of the Creative Commons CC BY license (https://creativecommons.org/licenses/by/4.0/), copyright © 2018, Chen et al., published by MDPI, no changes were made.

Similar to CL, LA has been used as a renewable feedstock to produce UV curable formulations either by itself[37,38] or in combination with other comonomers.[39] In one study, three-armed poly(D,L-lactide) (PDLLA) oligomers were end-functionalized with fumaric acid monoethyl ester to introduce double bonds in PDLLA for photopolymerization (Figure 12A).[38] Fumaric acid derivatives are attractive for functionalization as compared to (meth)acrylate groups since fumaric acid can be obtained from sugars in lignocellulosic biomass and is nontoxic.[17] To overcome the lower reactivity of fumarate oligomers as compared to methacrylate containing oligomers, a reactive comonomer was used to obtain crosslinked networks with gel contents >90%. Using SLA, porous gyroid structures could be fabricated from the PDLLA resins at high resolution as depicted in the SEM images in Figure 12B for application as tissue engineering scaffolds.

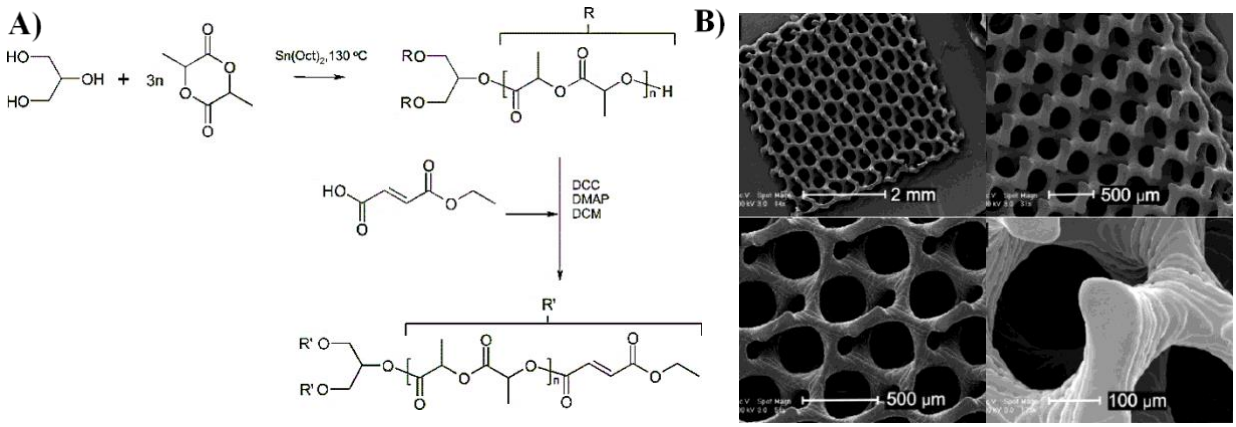

Figure 12: A) Synthesis of three-armed fumaric acid monoethyl ester functionalized PDLLA oligomers.[38] **B)** SEM images of SLA printed porous gyroid structures.[38] Reprinted with permission from {J. Jansen, F. P. W. Melchels, D. W. Grijpma and J. Feijen, Fumaric acid monoethyl ester-functionalized poly(D,L-Lactide)/N-vinyl-2- pyrrolidone resins for the preparation of tissue engineering scaffolds by stereolithography, *Biomacromolecules*, 2009, **10**, 214–220} Copyright {2009} American Chemical Society.

The studies described here reveal that renewably sourced cyclic esters such as CL and LA, can be synthetically modified with acrylate, methacrylate, or fumarate groups to develop sustainable 3D printing resins. These cyclic esters can be incorporated in 3D printing formulations in many ways: homopolymers with varying architectures (e.g. linear polymers and star polymers), copolymers with other cyclic ester comonomers, and blends of different types of homopolyesters. Depending on the molecular weight and architecture of the homopolymer, type of comonomer in the copolymer, and blending ratio of different homopolyesters, the properties of 3D printed parts can be easily tuned. In many cases, the hydrolytic sensitivity of the ester linkage has also been exploited to impart hydrolytic degradability. This is beneficial for a sustainable end-of-life of the 3D printed part and will be discussed in detail in section 2.2. Interestingly, the studies discussed in this section focus only on 3D printed parts intended for biomedical applications. Therefore, it is

crucial that this synthetic strategy is extended to other biomass-derived cyclic monomers such as tetrahydrofuran, caprolactam, or δ-valerolactone,[17] to potentially widen the scope of renewably sourced 3D printing resins beyond just biomedical applications.

1.1.1.3 Terpenes and Diacids

Diacids[17,40] and the terpene limonene,[17,41] have also been employed as renewable feedstocks in 3D printing. Diacids, can be obtained from lignocellulosic sugars through processes such as fermentation,[17,40] whereas limonene can be derived from citrus wastes such as orange peels.[17,41] However, not all terpenes can be directly derived from lignocellulosic biomass. It was recently demonstrated that terpenes other than limonene could be synthesized from lignocellulosic biomass using yeast (specifically *Rhodosporidium toruloides*).[42] Therefore, additional terpenes will be discussed in this section as they are an important class of renewable chemicals.[41] The major advantage of terpenes and diacids over other renewable feedstocks is that they serve as sources of double bonds in 3D printing compositions and they can be photopolymerized with either a monoacrylate or a thiol. Choosing the structure of the terpene, e.g. within an individual monomer, as shown in Figure 13A,[43] or within a polymer chain (e.g. linear or branched),[44] can allow for large variations in properties when photopolymerized with the same thiol (in this case a tetra-functional thiol, pentaerythritol tetrakis(3-mercaptopropionate)). For example, it was demonstrated that limonene based thermosets (Figure 13A) underwent plastic deformation and had a much higher strain at break and tensile strength (195% and 24 MPa, respectively) than geraniol based thermosets which deforms elastically and are more brittle (strain at break of 110% and a tensile strength of 2 MPa), as shown in Figure 13B.[43] In order to further understand the structure-property relationships of terpene-based materials, resins based on the terpene myrcene were synthesized in 3 different forms: monomer, linear polymer, and branched polymer.[44] It was demonstrated that the

linear polymers had an order of magnitude lower viscosity before printing and a higher elastic modulus (~ 15,000 Pa higher) after exposure to UV light than the branched counterparts.[44] Weems *et.al.* found that both of the myrcene polymer structures had a higher tensile strength and strain at break (~ 2.6 MPa and 120%, respectively) than the myrcene monomer (~ 2.3 MPa and 80%, respectively) and faster overall thiol-ene conversion when exposed to UV light. This indicates that the printing of terpenes could be improved through polymerization before UV curing.[44]

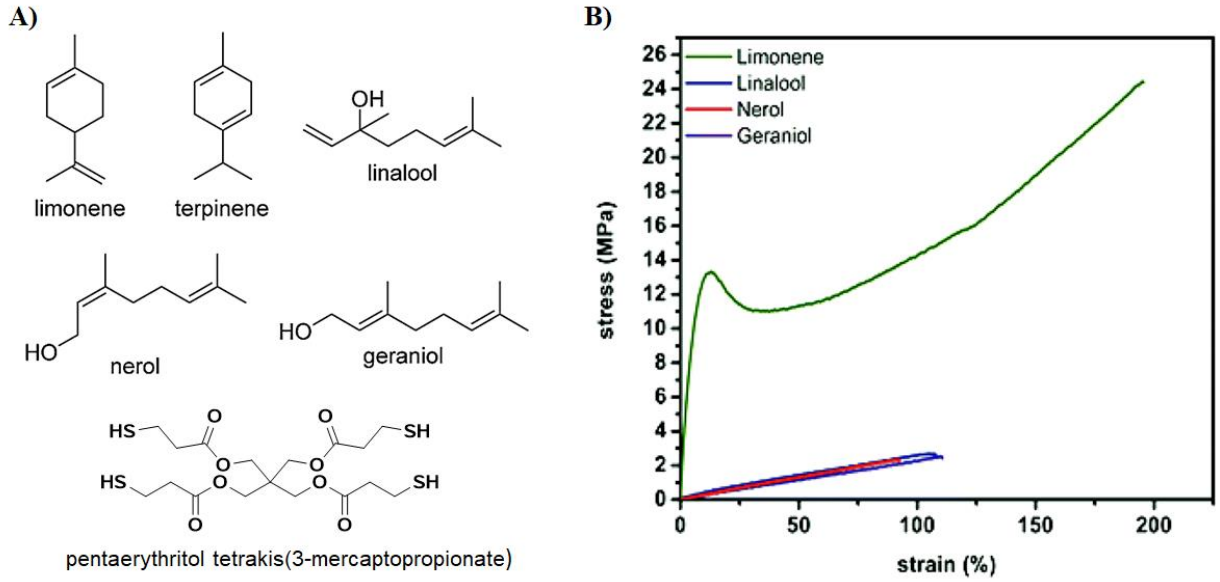

Figure 13: A) Chemical structures of different terpenes: limonene, terpinene, linalool, nerol, geraniol, and thiol: pentaerythritol tetrakis(3-mercaptopropionate) used in this study for thermoset synthesis.[43] **B)** Tensile stress vs strain curves of the different terpene based thermosets.[43] Reproduced from Ref. 43 with permission from the Royal Society of Chemistry.

Finally, diacids have also been used to produce photocurable polymers with co-monomers such as hydroxyethyl methacrylate (HEMA) or as multifunctional acrylates for photopolymerization. In one example, unsaturated polyesters were synthesized by the polycondensation reactions of different diacids and polyols. In this case, the following monomers were polymerized: diethylene glycol, propylene glycol, fumaric acid, and a choice of: isophthalic acid, adipic acid, sebacic acid, or succinic acid.[45] Post synthesis, the polymer was photocured with

HEMA to generate SLA printed materials with varying T_g, viscosity, and cell compatibility.[45] For example, the T_g could be varied from –39.94 °C to –2.48 °C just by changing from sebacic acid to isophthalic acid and slightly increasing the amount of fumaric acid in the polyester.[45]

In addition to unsaturated polyesters, diacids can be used to create short di- and tri-functional acrylate monomers as shown in Figure 14A.[46] In this example, glycidyl methacrylate was reacted with renewably sourced succinic and itaconic acids under solvent-free conditions to generate di-acrylate monomers.[46] An additional benefit of this synthetic technique was that the obtained di-acrylate monomers could be directly used without any purification steps, further eliminating the use of any additional chemicals. These materials could then be photopolymerized to form very intricate and precise structures with a DLP 3D printer. In this study, Miao *et.al.* evaluated both the heat deflection temperature (which assesses the ability of a material to maintain its shape under both heat and stress) and tensile properties, and found that thermosets from tri-functional itaconic acrylates had superior mechanical properties than those based on di-functional succinic acrylates, as shown below in Figure 14B-C.[46] For example, the heat deflection temperature was 50 °C higher (Figure 14B), and the tensile strength was 15 MPa higher for the tri-functional acrylate as compared to the di-functional variant (Figure 14C). [46] The authors believe this improvement in heat deflection temperature and tensile strength is due to the higher crosslink density of networks based on tri-functional acrylates.[46]

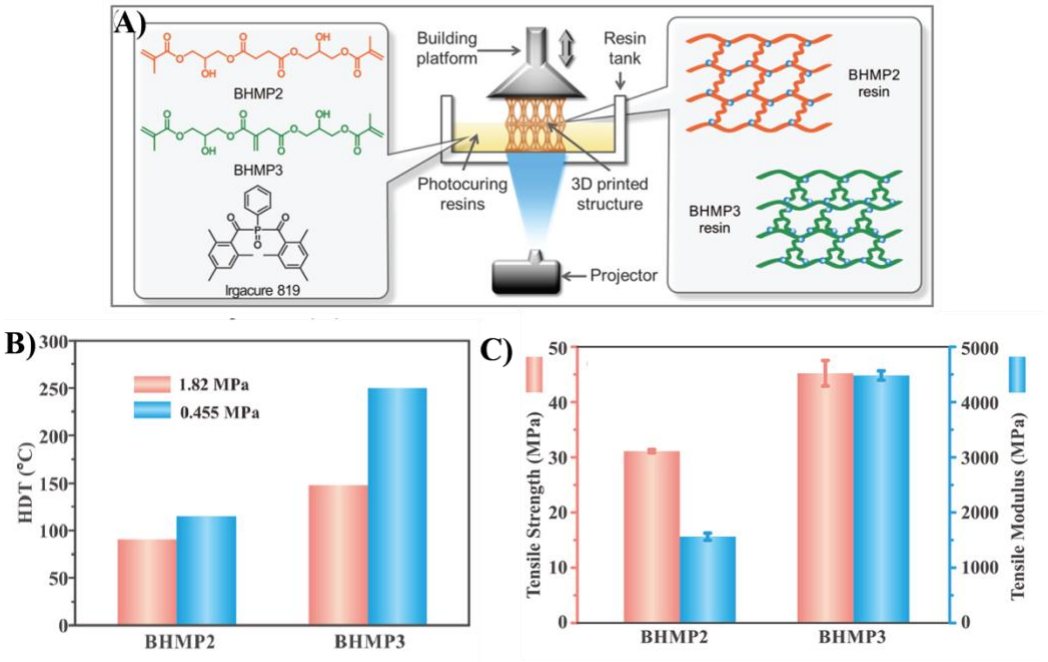

Figure 14: A) Process to photopolymerize di-functional and tri-functional acrylates obtained from diacids.[46] **B)** Heat deflection data for diacid based networks. BHMP2 is from the di-functional acrylate and BHMP3 is from the tri-functional acrylate.[46] **C)** Comparison of tensile strength and tensile modulus of the BHMP2 and BHMP3 resin.[46] Reprinted with permission from {J.-T. Miao, S. Peng, M. Ge, Y. Li, J. Zhong, Z. Weng, L. Wu and L. Zheng, Three-Dimensional Printing Fully Biobased Heat-Resistant Photoactive Acrylates from Aliphatic Biomass, *ACS Sustain. Chem. Eng.*, 2020, **8**, 9415–9424} Copyright {2020} American Chemical Society.

The examples described in this section reveal that limonene (and potentially other terpenes) and diacids can be used as renewable sources of double bonds in 3D printing resins. Due to the versatility in the structure of these feedstocks, the properties of 3D printed parts can be tuned from stiff to ductile. These materials can hence serve as sustainable replacements for a variety of commercially available 3D printing resins. However, further work comparing these renewable resins to commercial resins is necessary.

1.1.2 Vegetable Oils

Other important plant-based renewable sources such as linseed oils and soybean oils have also been utilized in 3D printing. Soybean oil is readily produced in the United States with the 2018-2019 annual production of 55 million metric tons, indicating that this renewable source is poised for potential large-scale use in multifunctional crosslinkers for 3D printing.[47] Linseed oil and soybean oil are very similar in structure as they are both triglycerides. The distinction between the two is based on the type and amount of the different unsaturated fatty acids present in the oils.[48,49] For the purposes of this review, the structure of the epoxidized oil shown in Figure 16A is considered to be similar for both the linseed oil and the soybean oil.

Epoxidized linseed oil has been utilized in cationic photopolymerization for SLA materials with di-epoxy crosslinkers to create 3D printing compositions.[50,51] However, linseed oil resins have slower curing kinetics than traditional resins. As an example, these linseed oil resins required 260 seconds of exposure time as compared to Formlabs clear resin and PR48, which only required 2 seconds of light exposure at identical wavelength and intensity.[51] In spite of this, these materials can reach 100 μm resolution with well-defined features that could potentially be used for biomedical applications.[51] Apart from this study, other examples of materials utilizing cationic photopolymerization can be found in these two reviews.[19,52] However, these studies do not necessarily demonstrate 3D printing or use of sustainable materials and hence are not discussed in this review.

Soybean oil has been functionalized with acrylates and used to produce 3D printing resins in several studies. Acrylated soybean oil has been used both with[53–55] and without[53,54,56] reactive diluents and a few specific examples are discussed below. For example, when acrylated soybean oil is used on its own with photoinitiator and printed on an SLA printer, the resulting material

demonstrates both biocompatibility and shape memory characteristics, as shown in Figure 15C.[56] The biocompatibility of the crosslinked soybean oil was found to be similar to both PCL and PLA, as demonstrated in the cell attachment and proliferation measurements below in Figure 15A-B. Furthermore, as compared to PCL and PLA, acrylated soybean oil facilitates processing without heat or reactive diluents since these soybean resins are liquids at room temperature.[56]

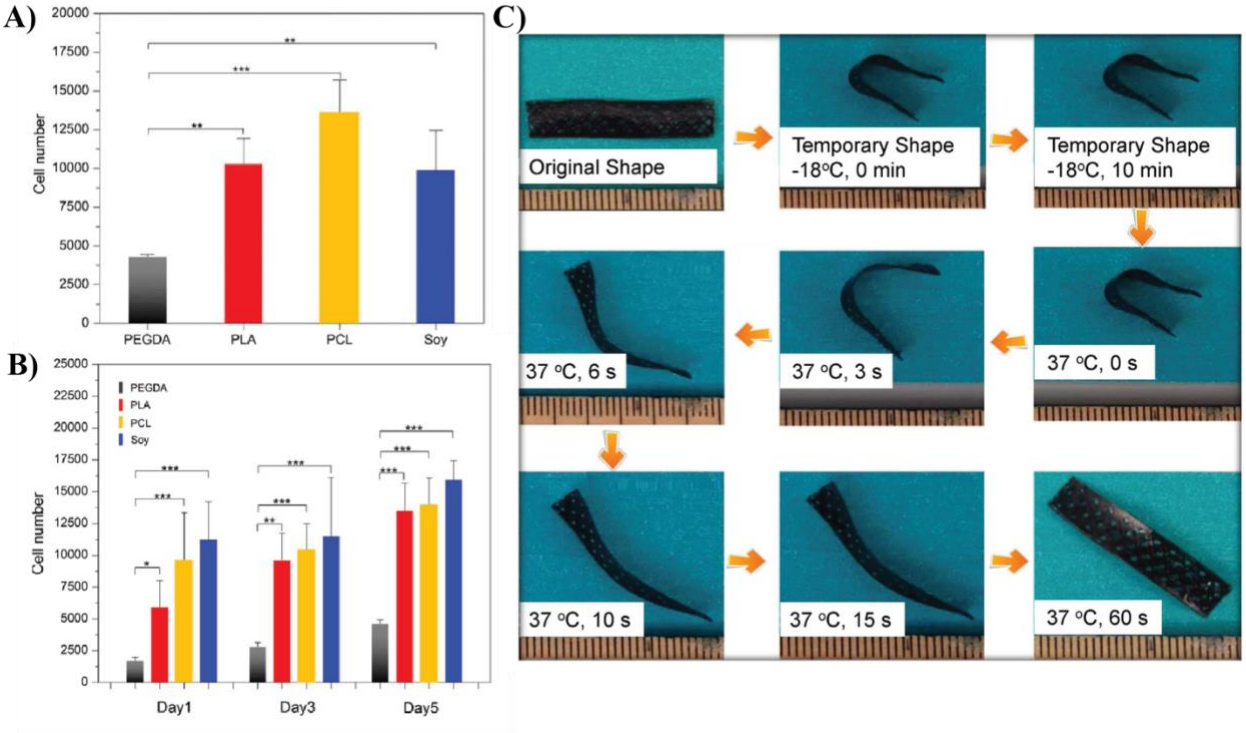

Figure 15: A) Cell attachment and **B)** cell proliferation measurements made on scaffolds created from different materials (PEGDA: polyethylene glycol diacrylate, PLA: polylactide, PCL: polycaprolactone, and soy: soybean oil).[56] **C)** Demonstrations of shape memory characterstics.[56] Reproduced from Ref. 56 under the terms of the Creative Commons CC BY license (https://creativecommons.org/licenses/by/4.0/), copyright © 2016, Miao et al., published by Springer Nature, no changes were made.

In another study, acrylated or methacrylated soybean oil was mixed with a maximum of 40% isobornyl methacrylate (IBMA), which acts as reactive diluent.[55] The authors evaluated the effect of acrylate type (methacrylate vs acrylate) and the degree of methacrylate functionality on

the final 3D printed visual quality and mechanical properties. The authors created three different resin solutions: acrylated soybean oil with IBMA, methacrylated soybean oil with IBMA, and methacrylated soybean oil with a lower degree of methacrylation with IBMA (synthesis of methacrylated soybean oil is shown in Figure 16A).[55] Visually, these materials had similar definition of the 3D printed features, but materials with a greater concentration of methacrylate groups had a darker amber color as seen in Figure 16B(b). Tensile properties also demonstrated the structure-property relationship differences between the resins. For example, changing from an acrylate to a methacrylate increases the tensile strength from 36 MPa to 44 MPa and the Young's modulus from 870 MPa to 1000 MPa, respectively.[55] Therefore, by changing the nature of the acrylate, the properties of the resin can be varied to create a stiffer material. In comparison to the strain at break and toughness of commercial resins PR48 (~ 2% and 20 J/m^{-3}, respectively) or Liqcreate Deep Blue (LCDB, ~7% and 294 J/m^{-3}, respectively), the soybean derived resins have a much higher strain at break and toughness varying from ~21% to ~9.5% and 323 to 560 J/m^{-3}, respectively.[55] This suggests that soybean oil based materials can be used for applications that require higher toughness than the evaluated commercial materials.[55]

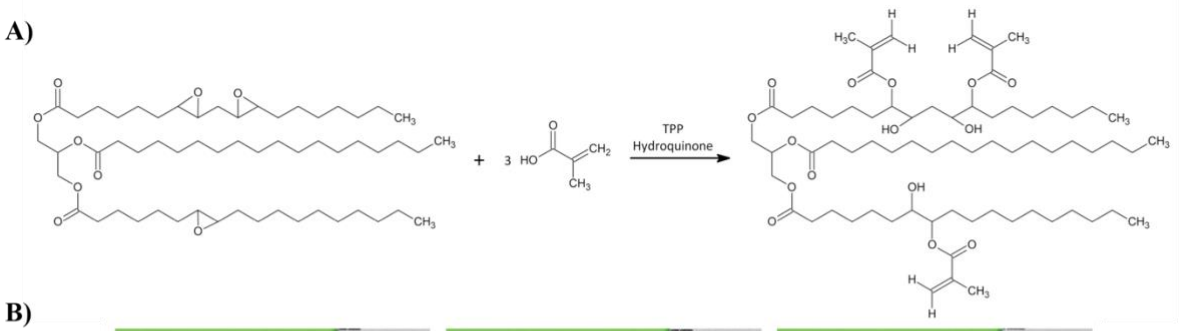

Figure 16: A) Synthesis of methacrylated soybean oil (Triphenylphosphine, TPP).[55] **B)** Demonstrations of 3D printing with soybean oil and isobornyl methacrylate (IBMA). (a) 40 wt% IBMA and 60 wt% acrylated soybean oil (b) 40 wt% IBMA and 60 wt% methacrylated soybean oil (c) 40 wt% IBMA and 60 wt% methacrylated soybean oil (lower degree of methacrylate functionality than formulation (a)).[55] Reprinted with permission from {J. Guit, M. B. L. Tavares, J. Hul, C. Ye, K. Loos, J. Jager, R. Folkersma and V. S. D. Voet, Photopolymer Resins with Biobased Methacrylates Based on Soybean Oil for Stereolithography, *ACS Appl. Polym. Mater.*, 2020, **2**, 949–957} Copyright {2020} American Chemical Society.

Overall, these studies suggest that both linseed oil and soybean oil can be successfully used in 3D printing resins to print parts with tunable properties. These oil-based resins can photopolymerize by themselves or when mixed with renewable reactive diluents, leading to fully renewably sourced resins. Many of these oil-based materials have been compared to commercial materials such as Formlabs clear resin and PR48 in terms of properties. However, these materials are generally more ductile than the commercial counter parts.

1.1.3 Animal Products and Other Sources

Apart from the many different plant-based products that have been discussed up to this point, animal products have also been utilized as renewable feedstock for 3D printing. While this section focuses on animal based products, a few of these feedstock chemicals can be derived from other sources as well, for example, polyamines (which can be produced from proteins in vegetables, meat, and dairy)[57] and alginate (which can be derived from both algea[58] and bacteria[59,60]). Other renewable chemicals that have been incorporated in 3D printed resins that are primarily produced from animals include hyaluronic acid (found in the extracellular matrix of different animal tissues and can be produced by bacteria),[61] silk fibroin (fiber produced from

silkworms),[62] globular proteins (isolated from cell plasma),[63] gelatin (derived from collagen[64], however, gelatin will not be discussed here in detail as it has been reviewed recently),[65] and keratin (found in many animal tissues). This section will look at how these chemicals are used to create sustainable resins for 3D printing. For a quick overview of what materials are discussed in this section please see Table 1.

Polyamines are produced from amino acids found in vegetables, meat, and dairy as can been seen in a review on the production of biogenic amines.[57] In several studies, polyamines have been incorporated to form di-urethanes with two methacrylate end-groups, which can be further photopolymerized via free radical chemistry[66] or thiol-ene[67] click chemistry. Pyo *et.al.* synthesized isocyanate-free aliphatic di-urethane monomers with methacrylate groups for crosslinking.[66] In this study, they utilized the technique of ring-opening polymerization to form the urethane bond by copolymerizing a cyclic carbonate with different polyamines (Figure 17A). With this synthetic route, the authors were able to eliminate the use of hazardous isocyanates and phosgene. It is worth noting that isocyanates are known to be highly toxic to human health and are also derived by reacting amines with highly toxic phosgene derivatives.[66] Hence, this isocyanate-free polyurethane synthesis approach enhances the sustainability of 3D printing polyurethane resins.[66,67]

Pyo *et.al.* also demonstrated that the six-membered cyclic carbonate used in the synthesis of polyurethanes can be obtained via a solvent-free and catalyst-free technique.[68] In addition, the ring opening polymerization reaction is also initiated by heat, avoiding the use of catalysts and solvents.[66,67] By manipulating the choice of polyamine (i.e. Putrescne, Cadaverine, Spermidine, and Spermine, as shown in Figure 17A), the light exposure time,[66] or the thiol compound,[67] the resulting material stiffness could be widely tuned.[66] By changing the polyamine and the exposure time, the stiffness could be tuned from < 5 MPa to 20 MPa, as shown in Figure 17B.[66] The authors

believe that spermine has the highest stiffness due to the two secondary amines participating in forming the di-urethane, promoting smaller chains and reducing the flexibility of the networks.[66] In addition, these polyurethane networks demonstrated high cell viabilities, through a cell cultivation test, of more than 95% even after 7 days, suggesting that these materials can be a sustainable option for biomedical applications.[66]

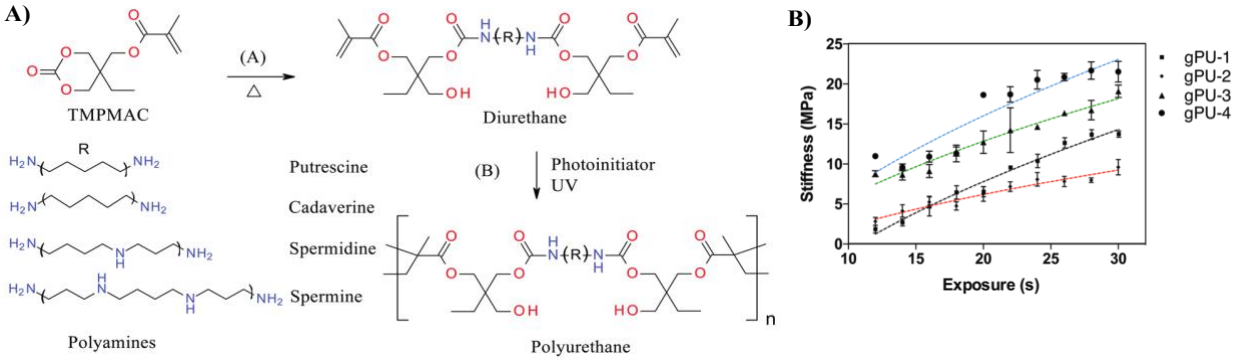

Figure 17: A) Synthesis of polyurethanes from different amines where step (A) indicates the addition of the polyamine to ring open the cyclic carbonate monomer and step (B) indicates the UV polymerization reaction occurring.[66] **B)** Stiffness vs exposure time of different polyurethane networks. gPU-1: Putrescine, gPU-2: Cadaverine, gPU-3: Spermidine, gPU-4: Spermine.[66] Reprinted with permission from {S. H. Pyo, P. Wang, H. H. Hwang, W. Zhu, J. Warner and S. Chen, Continuous optical 3D printing of green aliphatic polyurethanes, *ACS Appl. Mater. Interfaces*, 2017, **9**, 836–844} Copyright {2017} American Chemical Society.

Apart from forming new acrylates that incorporate polyamines, a commercial amino resin with reactive acrylate groups has also been mixed with HEMA, photoinitiator, and other additives to form a resin that can be 3D printed.[69] While it is unclear if the commercial amino resin is biobased, this study demonstrated that dopamine (another biogenic amine) could be used as a biobased light absorber in this resin.[69] Light absorber additives are typically added to SLA/DLP compositions to help improve the feature quality and prevent overcure during light exposure.[70]

This suggests that dopamine could potentially replace light absorbers in traditional resins to allow for a biobased alternative.

Silk[62] and globular proteins have also been incorporated into 3D printing compositions.[71] Both silk[62] and a particular globular protein[71] (bovine serum albumin) have functional groups allowing for methacrylate functionality to produce sustainably derived crosslinkers. Silk, for example, has primary amine groups that have been methacrylated using glycidyl methacrylate.[62] The methacrylated silk can then be photopolymerized without any co-monomers in the presence of cells, allowing 3D printing with cells *in-situ.*[62] Hong *et.al.* determined that cell viability and cell growth was not disrupted on these silk methacrylate materials even after photopolymerization.[62] This silk based thermoset was also evaluated via three-point bending studies with the goal of replacing a rabbit trachea. It was demonstrated that the flexural properties of the silk with cells (max displacement of > 2 mm and max loading force of 70 gram-force (gf)) were better than that of the rabbit trachea (max displacement of < 1.5 mm and max loading force of 20 gf). Furthermore, the properties continued to improve after an additional week of cell cultivation.[62]

While the silk was printed with cells *in-situ*, the 3D printed materials made from methacrylated bovine serum albumin crosslinker cultured cells after printing and showed cell viability of greater than 95%, even when mixed with small amounts (1-10%) of a polyethylene glycol di-acrylate or acrylate additive.[71] In this study, the hydroxyl groups of the globular protein BSA were methacrylated using methacrylic anhydride in an aqueous salt buffer solution, thereby replacing organic solvents with alternative benign solvents.[71] In addition to cell viability studies, these 3D printed globular protein networks demonstrated different properties in both the swollen and dehydrated state, as discussed below and demonstrated in Figure 18B. In both the swollen and dehydrated cases, the compressive strength of these networks increased after thermal treatment, as

thermal treatment causes the protein to denature, increasing the intermolecular interactions within the crosslinked structure as seen in the far right image in Figure 18A.[71] In the case of the swollen hydrogel, the compressive strength of the material increased by only 1-2 MPa after thermal treatment; however, in the case of the dehydrated network, the compressive strength increased by hundreds of MPa as seen in Figure 18B moving from pre-thermal treatment (left) to post-thermal treatment (right). Both the tensile studies and the cell viability studies demonstrate that these globular proteins can be used to create precisely designed parts with tunable properties (depending on the co-monomer) and high cell viability. These traits make this resin useful for biomedical applications; specifically, the authors draw attention to load bearing biomedical devices.[71] Furthermore, this study also took advantage of the enzymatic sensitivity of the protein BSA to introduce biodegradability in the 3D printed part. Enzymatic degradation of SLA printed BSA networks with and without a PEG di-acrylate comonomer was evaluated by immersing them in a solution containing the enzyme proteinase K. Importantly, methacrylated-BSA networks (with no comonomer) that were irradiated with UV light and thermally treated, were completely digested by proteinase K within 16 hours.[71]

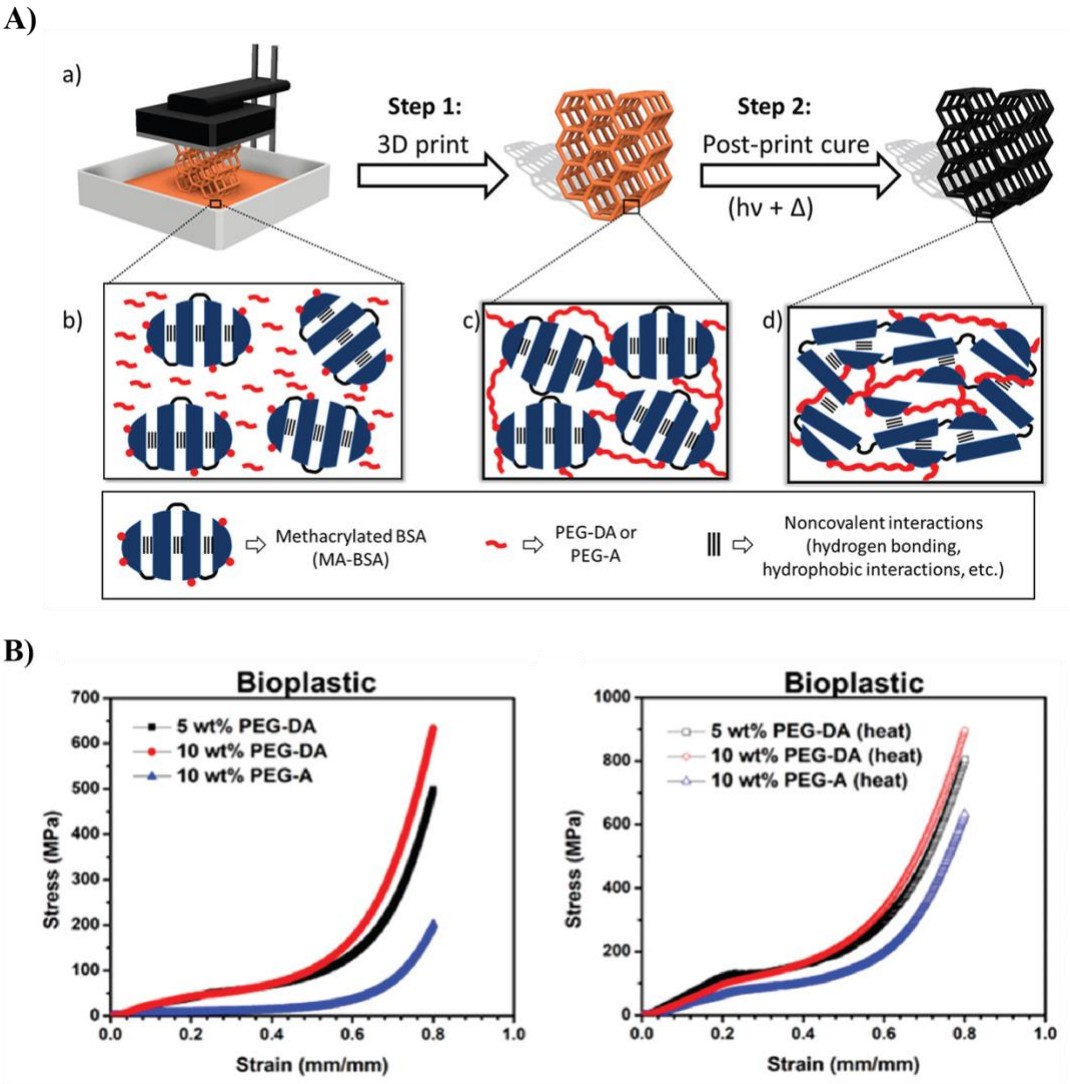

Figure 18: A) (a**)** Schematic of the 3D printing process and post processing steps. (b) Resin composition (BSA: bovine serum albumin) (c) Schematic depicting network structure after photopolymerization. (d) Network structure after heating to denature the protein.[71] **B)** Compressive stress vs strain curves for BSA mixed with either PEG di-acrylate (PEG-DA) or PEG acrylate (PEG-A) for the material as a hydrogel (left graph) and the material after heat treatment denaturing the protein (right graph).[71] Reprinted with permission from {P. T. Smith, B. Narupai, J. H. Tsui, S. C. Millik, R. T. Shafranek, D.-H. Kim and A. Nelson, Additive Manufacturing of Bovine Serum Albumin-Based Hydrogels and Bioplastics, *Biomacromolecules*, 2020, **21**, 484–492} Copyright {2020} American Chemical Society.

Other animal products such as hyaluronic acid, alginate, and keratin have also been incorporated into 3D printing compositions. Hyaluronic acid has been typically added to 3D printing formulations to decrease toxicity effects of the printed materials to the cells. However, the study conducted by Shie *et.al.* suggests that adding 0.5% hyaluronic acid to the 3D printing resins can modulate physical properties as well. For example, the Young's modulus of the printed part increases from 30 MPa to 40 MPa with the addition of 0.5% hyaluronic acid.[72] The authors attribute this increase in modulus to the hyaluronic acid reacting or interacting with the polyurethanes to create a tighter network.[72] This suggests that hyaluronic acid could be utilized as a sustainable additive in 3D printing for biomedical applications to maintain cell viability as well as to improve the strength of the material.

While hyaluronic acid is just an additive to a photopolymerizable resin, alginate[73] and keratin[74] can be used as the primary curable component in 3D printing compositions. In a recent study by Valentin *et.al.*, 3 wt% alginate in a dilute PBS solution was crosslinked under UV light using a photoacid generator and a cation to form an ionic network, as shown in Figure 19A.[73] The crosslinks can then be reversed by immersing the network in ethylenediaminetetraacetic acid, which acts as a chelating agent to remove the ions (Figure 19A). In this study, the 3D printed pattern was evaluated based on the amount and type of crosslinking ion chosen to find the best combination for precise 3D printing resolution as shown in Figure 19B. The degradation of the crosslinks was also evaluated based on the type and amount of ion. Overall, Valentin *et.al.* found that using calcium ions allowed for fast degradation kinetics with little overcure of the 3D printed part. This study indicates that alginate can be used to create renewably sourced thermosets with tunable printing and degradation properties.

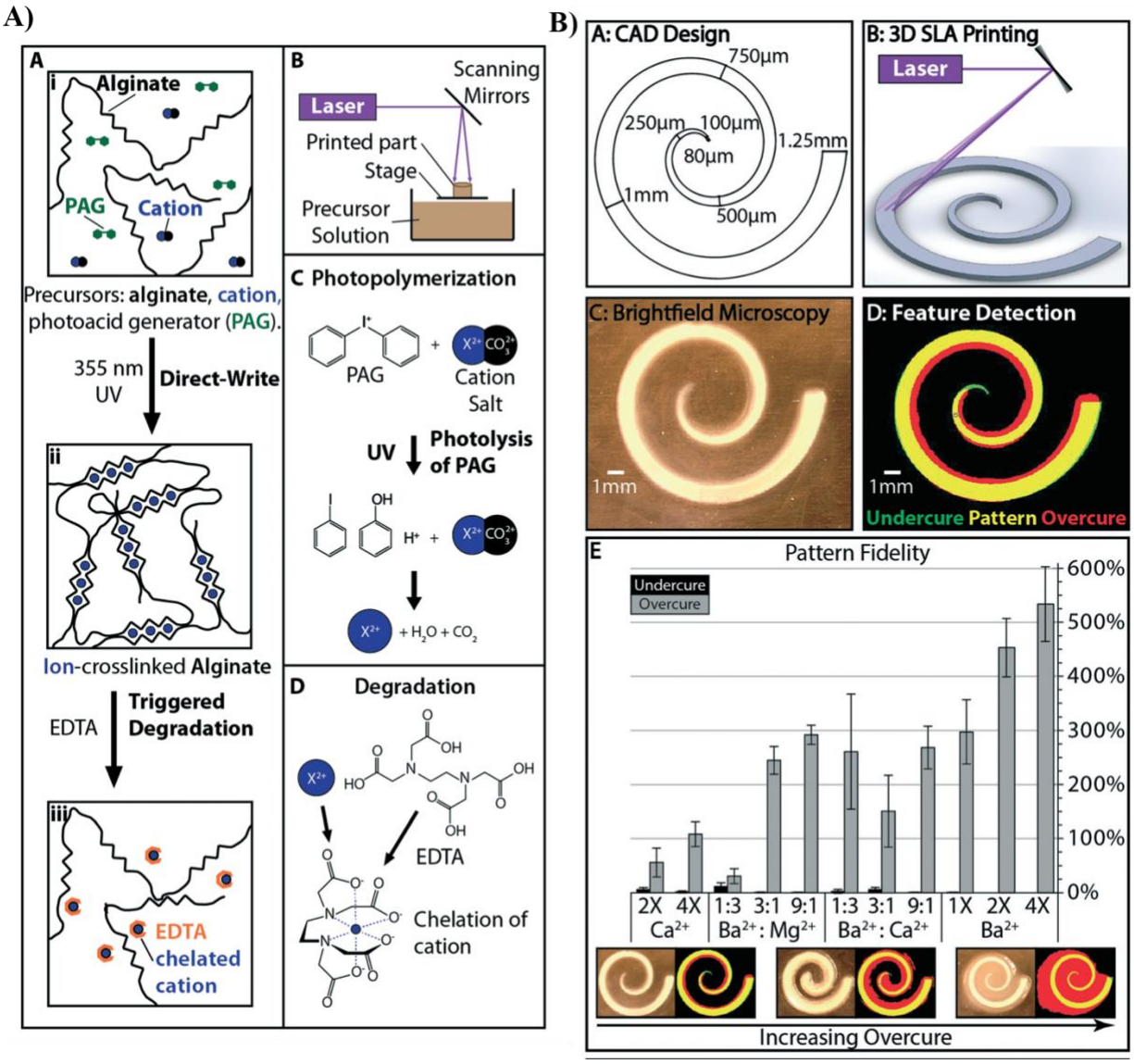

Figure 19: A) (a) Schematic depicting alginate crosslinking with a cation and photoacid generator and crosslink degradation with a chelating cation. (b) 3D printing mechanism. (c) Photopolymerization chemistry. (d) Degradation mechanism.[73] **B)** (a) Spiral design. (b) 3D printing schematic. (c) Microscopy image of printed spiral. (d) Depiction of how the different features of undercure, overcure, and regular pattern were detected and characterized. (e) Quantitative pattern fidelity based on amount and type of cation (1x is defined as 0.18, the molar

ratio of cation to carboxyl groups on the alginate).[73] Reproduced from Ref. 73 with permission from the Royal Society of Chemistry.

Similar to alginate, keratin has also been utilized for 3D printing at less than 10 wt% concentration in a PBS buffer solution.[74] In addition to using keratin, Placone *et.al.* also included an initiator, catalyst, and inhibitor in the formulation and demonstrated that the initiator and inhibitor could be bioderived using riboflavin and hydroquinone, respectively, giving alternatives to traditional inhibitors and initiators that are not generally bioderived.[74] Mechanical property testing of this formulation showed that the compression modulus increased from 5.49 kPa to 15.45 kPa as the amount of keratin was increased from 4% to 6% (wt/vol), demonstrating that network stiffness can be increased by increasing the amount of keratin.

As described in this section, many different animal or other organism-based products can be used in 3D printing formulations as sustainable main components or sustainable additives such as initiators, inhibitors, and light absorbers. One key aspect of materials based on this type of renewable feedstock is that they exhibit cell compatibility, making them desirable for biomedical applications. Future work could focus on comparing the properties of these sustainable formulations with traditional SLA/DLP resins to evaluate their suitability for non-biomedical applications.

1.2 Waste Feedstock

Apart from renewable feedstock, waste feedstock is also very important when considering sustainability. Using waste as a feedstock for 3D printing potentially allows for "upcycling" of materials that would traditionally go unused and be discarded, thereby harming the environment through mismanaged waste. Two examples of waste feedstock that have been incorporated into SLA materials include waste cooking oil and carbon dioxide (CO_2).

In a recent study, waste cooking oil was demonstrated to be useful in producing SLA resins.[75] The waste cooking oil from the McDonalds restaurant chain comprises mostly of triglycerides, which are essentially unsaturated fatty acids as shown in Figure 20A.[75] Taking advantage of the unsaturation in the triglyceride, Wu *et.al.* utilized a reaction with acrylic acid and boron trifluoride etherate to functionalize the triglycerides with acrylate groups in a solvent-free synthesis, as shown in Figure 20A. Interestingly, the only purification of the waste cooking oil that was necessary before the reaction was to filter the waste cooking oil to remove any large particles.[75] These oils with pendent acrylate groups could be used to generate a photopolymerizable resin by incorporating just 1% photoinitiator.[75] 3D printing was demonstrated on a Solus DLP printer to create thermosets from this traditionally wasted oil, as shown in Figure 20B. Notably, Wu *et.al.* also demonstrated that the unused acrylic acid and catalyst from the functionalization reaction could be recovered and reused.[75] In addition, the solvents added during the purification step could also be recovered and reused again in future syntheses. These steps make the waste cooking oil-based UV formulations more sustainable by preventing material waste.

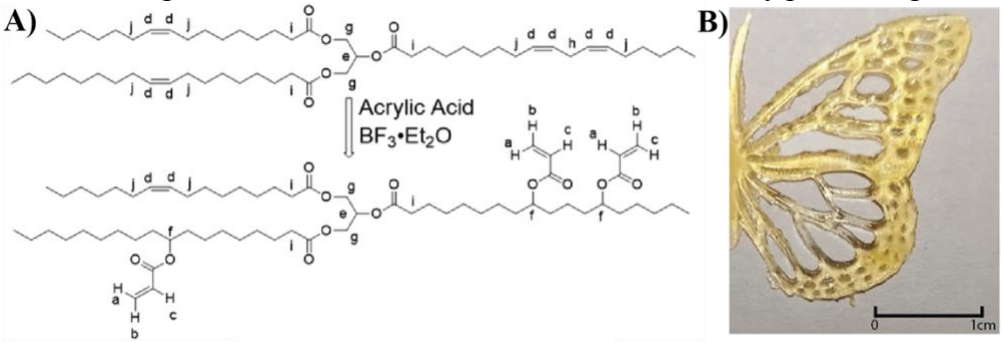

Figure 20: A) Reaction scheme to functionalize waste cooking oil with acrylate groups.[75] **B)** Image of part printed with the waste cooking oil.[75] Reprinted with permission from {B. Wu, A. Sufi, R. Ghosh Biswas, A. Hisatsune, V. Moxley-Paquette, P. Ning, R. Soong, A. P. Dicks and A. J. Simpson, Direct Conversion of McDonald's Waste Cooking Oil into a Biodegradable High-

Resolution 3D-Printing Resin, *ACS Sustain. Chem. Eng.*, 2020, **8**, 1171–1177} Copyright {2020} American Chemical Society.

This study also took advantage of the enzymatic sensitivity of fat molecules to impart biodegradability to the 3D printed parts. Interestingly, the biodegradation of the printed network was evaluated by a soil burial test, where the thermoset was buried 50 mm under the soil surface at 30% relative humidity and at 25 °C. The degradation test revealed that the thermoset underwent ~25% mass loss within 2 weeks.[75] This was due to the presence of bioavailable fat molecules in the printed material which can be biodegraded in the soil.

CO_2 is another major waste feedstock of interest in 3D printing. In a recent study, CO_2 was used to synthesize a cyclic carbonate with a pendent methacrylate, which was further ring-opened with an amine to obtain a photopolymerizable di-methacrylate urethane (Figure 21). This di-methacrylate urethane synthesis was performed under solvent-free conditions and without the use of isocyanates.[76] This particular process allows for CO_2 to be used in 3D printing materials when it would otherwise end up in the atmosphere. Furthermore, this process also eliminates the use of highly toxic isocyanates in polyurethane synthesis, thereby making the process greener. Depending on the choice of amine group within the biobased urethane acrylate the mechanical properties could be modified. For example, tensile strength ranged between 20.5 and 85 MPa demonstrating the wide range of properties that can be obtained by altering the amine group.[76] This range of tensile strength values also incorporates a commercial resin (Laromer), which has a tensile strength of 71.9 MPa.[76] In addition, the strain at break could be manipulated from 90% to 1.2%, which encompasses the strain at break of the commercial material at 6%.[76] These results demonstrate that the properties of these polyurethanes can be tuned from stiff to ductile, and hence they can serve as potential sustainable replacements for multiple commercial resins.

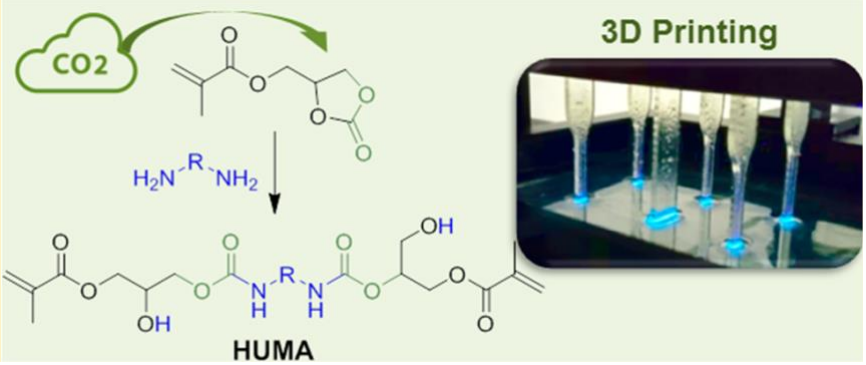

Figure 21: Left: Synthetic scheme showing sequestering of CO_2 and production of the di-methacrylate urethane with different amines. Right: Image demonstrating 3D printing of resins composed of: 4-methacryl-oylmorpholine, HUMA, and photoinitiator (diphenyl(2,4,6-trimethylbenzoyl)-phosphine oxide).[76] Reprinted with permission from {V. Schimpf, A. Asmacher, A. Fuchs, B. Bruchmann and R. Mülhaupt, Polyfunctional Acrylic Non-isocyanate Hydroxyurethanes as Photocurable Thermosets for 3D Printing, *Macromolecules*, 2019, **52**, 3288–3297} Copyright {2019} American Chemical Society.

The use of waste cooking oil and the sequestering of CO_2 indicate that waste materials can be successfully used in SLA 3D printing processes and, as the CO_2 study demonstrates, they can even have competitive properties. Notably, the waste cooking oil investigation demonstrates an important mode of degradation by using soil burial tests. Future work understanding the details of soil degradation, characterizing degradation products, and understanding environmental impact is important for evaluating sustainability; these topics will be discussed further in section 3.3. Further work in this area of waste feedstocks can push the sustainability of SLA materials by effectively upcycling waste into 3D printed objects.

2. End-Of-Use

While feedstock selection is very important when considering sustainability, evaluating material end of life is equally important. There are many different sustainable end-of-life

possibilities for materials, however, there are two in particular that have been used for SLA/DLP 3D prints. These sustainable end-of-use possibilities are: 1) materials that can be reprocessed and used again in 3D printing or in another plastic process such as remolding, and 2) degradable materials that can degrade under applied stimulus, such as a pH change.

2.1 Reprocessable Materials

Reprocessability refers to materials that can be remolded for reuse in 3D printing or other applications. Reuse of these materials prevents landfilling after end-of-life. One difficulty with SLA 3D printed materials is that they are typically thermosets. The chemical crosslinks in these thermosets can prevent them from being reprocessed. A few reprocessing methods that have been explored include 3D printing thermoplastics and utilizing covalent adaptable networks that enable reprocessing via transesterification and diels-alder linkages.

2.1.1 Thermoplastics

As mentioned in the introduction, thermoplastics are readily used in FDM 3D printing. As thermoplastics can be remolded with heat, they can be readily reprocessed. In contrast to FDM, forming thermoplastics in SLA/DLP 3D printing is rare. While there are some drawbacks to thermoplastics, such as the lack of solvent resistance, the benefits of being able to reprocess them could be a major advancement for those applications that do not need solvent resistance. 3D printing of thermoplastic polymers has been demonstrated using both thiol-ene click chemistry and free radical polymerization using UV light.

The most recent example utilizes thiol-ene click chemistry to form crystalline polymers with high toughness (102 MJ/m^{-3}).[77] The monomer mixture for this process was a 1:1 ratio of 1,6-hexane di-thiol and di-allyl terephthalate with photoinitiator (monomer structures shown in Figure 22A). Due to the step-growth nature of thiol-ene click chemistry and associated rapid

photopolymerization kinetics, high molecular weight linear polymers were formed.[77] The aromatic polyester chains crystallized after about eight minutes, as shown in Figure 22B.[77] The thermoplastic nature of this material allowed the 3D printed part to be heated and reshaped, as shown in the time lapse photos of Figure 22C, demonstrating reprocessability.[77]

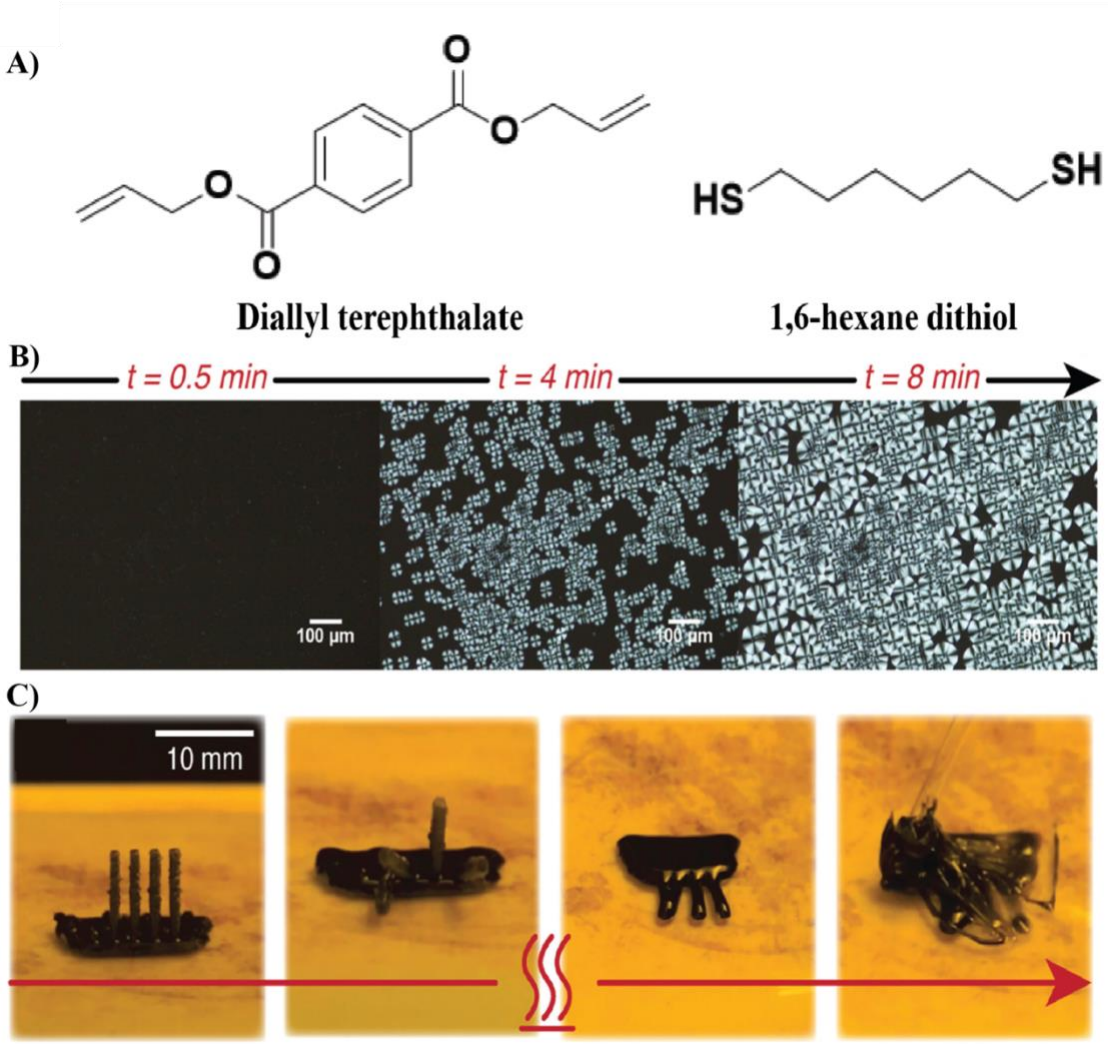

Figure 22: A) Monomers used in the synthesis of photopolymerizable thermoplastic. **B)** Image series demonstrating the timescale and type of crystals that form from the polymer chains.[77] **C)** Image series from a video which demonstrates the thermo remolding process as the shape is heated, flows, and then manipulated with a glass pipette to reshape it.[77] Panel A adapted from Ref.77 with

permission from the Royal Society of Chemistry. Panels B and C Reproduced from Ref. 77 with permission from the Royal Society of Chemistry.

Another example of an SLA thermoplastic utilized conventional free radical polymerization to form a high T_g thermoplastic. Free radical polymerization of 4-acryloylmorpholine using UV light creates a linear polymer with a T_g of 155 °C.[78] The photopolymerization kinetics of this resin are very similar to that of a commercial thermoset resin system, as indicated in Figure 23B, suggesting it could be readily implemented into 3D printing processes. The photopolymerization to produce this thermoplastic relies on the ability of the polymer to rapidly phase separate from the monomer. The rapid phase separation during polymerization allows for precise printing resolution, as demonstrated by Figure 23C-E.[78] The main use of this thermoplastic is for molding other materials, as this polymer can be dissolved in water preventing the use of harsh organic solvents.[78] While this study did not directly demonstrate remolding of the printed part through heating, it is expected to be possible.

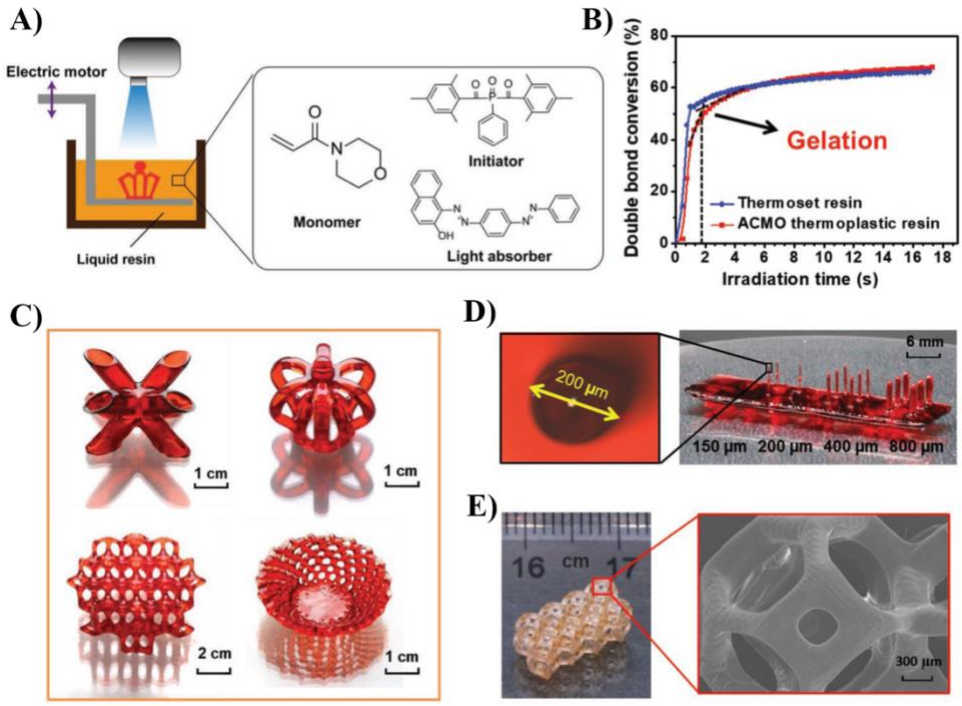

Figure 23: A) Resin mixture of monomer, initiator, and light absorber in representative DLP schematic.[78] **B)** Irradiation time vs double bond conversion comparing the rates between the thermoplastic monomer formulation and a commercial resin (FSL-C from S-MAKER).[78] **C)** Examples of 3D printed parts from monomer formulation.[78] **D)** Resolution test of different pillar sizes, authors note that all 150 μm pillars and half of the 200 μm pillars collapsed.[78] **E)** Demonstration of fine lattice structures.[78] Reprinted with permission S. Deng, J. Wu, M. D. Dickey, Q. Zhao and T. Xie, Rapid Open-Air Digital Light 3D Printing of Thermoplastic Polymer, *Adv. Mater.*, 2019, **31**, 1903970. Copyright © 2019 WILEY-VCH Verlag GmbH & Co. KGaA, Weinheim.

Ultimately, these examples highlight that thermoplastic materials can be 3D printed via SLA/DLP processes through careful consideration of the monomer chemistry. Thermoplastics can dramatically change traditional SLA/DLP materials because they allow for remoldable and, therefore, recyclable 3D printed parts. Reprocessability through remolding ultimately allows the reduction of plastic waste by preventing parts from being immediately landfilled after printing. One drawback of thermoplastics is their lack of solvent resistance. However, dissolution in solvents could introduce an opportunity to break into the casting/molding industry that SLA/DLP printing already serves. The casting industry relies on making 3D printed parts as molds for other material castings. The mold, produced from SLA/DLP materials, is traditionally burned or cut away from the casting. Alternatively, thermoplastics could readily assist this industry by offering materials that can be easily removed with solvent. Additionally, these materials can also be remolded to fix fine detail, or even remolded if a mistake is made while 3D printing the mold. Future work expanding the range of thermoplastics that can be printed with SLA/DLP will be important for further sustainability advancements.

2.1.2 Covalent Adaptable Networks (CANs)

The second method of reprocessing involves incorporating exchangeable or reversible bonds in crosslinked materials to produce CANs. These exchangeable or reversible bonds allow the material to be remolded with heat thereby introducing reprocessability. One example of a CAN included in this section incorporates exchangeable bonds in SLA 3D printing, while the other incorporates bonds that can disassociate. One important note is that similar to thermoplastics from SLA/DLP processes, the reprocessability of CANs enables thermal remolding, but not recycling back into the SLA/DLP process. However, thermal remolding is an important recycling possibility that could prevent SLA/DLP parts from ending up in waste streams.

In the first example, exchangeable ester bonds with pendant hydroxy groups have been employed for 3D printing, which can be rearranged through transesterification. The transesterification rearrangement is best illustrated in Figure 24 panels c-g which depict that heating allows for the exchange of bonds. This exchange of bonds gives the material the ability to be remolded into a new shape leading to reprocessable networks. The common crosslinker used for these transesterification reactions is bisphenol A glycerolate di-(meth)acrylate that contains both ester bonds and pendent hydroxy groups as shown in Figure 24(b). This reagent has been shown to be useful for transesterification reactions with a second crosslinker containing ester bonds (1,4 – butanediol dimethacrylate),[79] and in a co-polymerization reaction with an acrylate monomer containing ester bonds and hydroxy groups (2-hydroxy-3-phenoxypropyl acrylate),[80] as indicated in Figure 24b. The (meth)acrylate groups in these compounds allow for photopolymerization when mixed with a photoinitiator to generate the initial 3D printed part. Next, thermal reprocessing of these materials can be done either with (as shown in Figure 25A)[80] or without[79] an added catalyst. These studies demonstrate that the 3D printed CANs could be

thermally recycled three times while maintaining similar tensile properties, as shown in Figure 25B, where the tensile strength ranges from 15 MPa to 11 MPa, and the strain at break varies from 8% to 4%.[80] In addition, these studies also demonstrate that properties could be varied depending on the recycling conditions (e.g. heat, pressure, and time).[79] For example, the tensile strength could be varied from 14 MPa to 16 MPa just by changing the pressure during molding from 9 MPa to 12 MPa at constant processing time and temperature.[79] The tensile strength and strain at break were then further increased by increasing the processing temperature to 200 °C from 150 °C, to obtain a strain at break of 4.5% and a tensile strength of 22 MPa.[79] Therefore, these 3D printed CANs can be reprocessed and the mechanical properties can be varied depending on the reprocessing conditions.

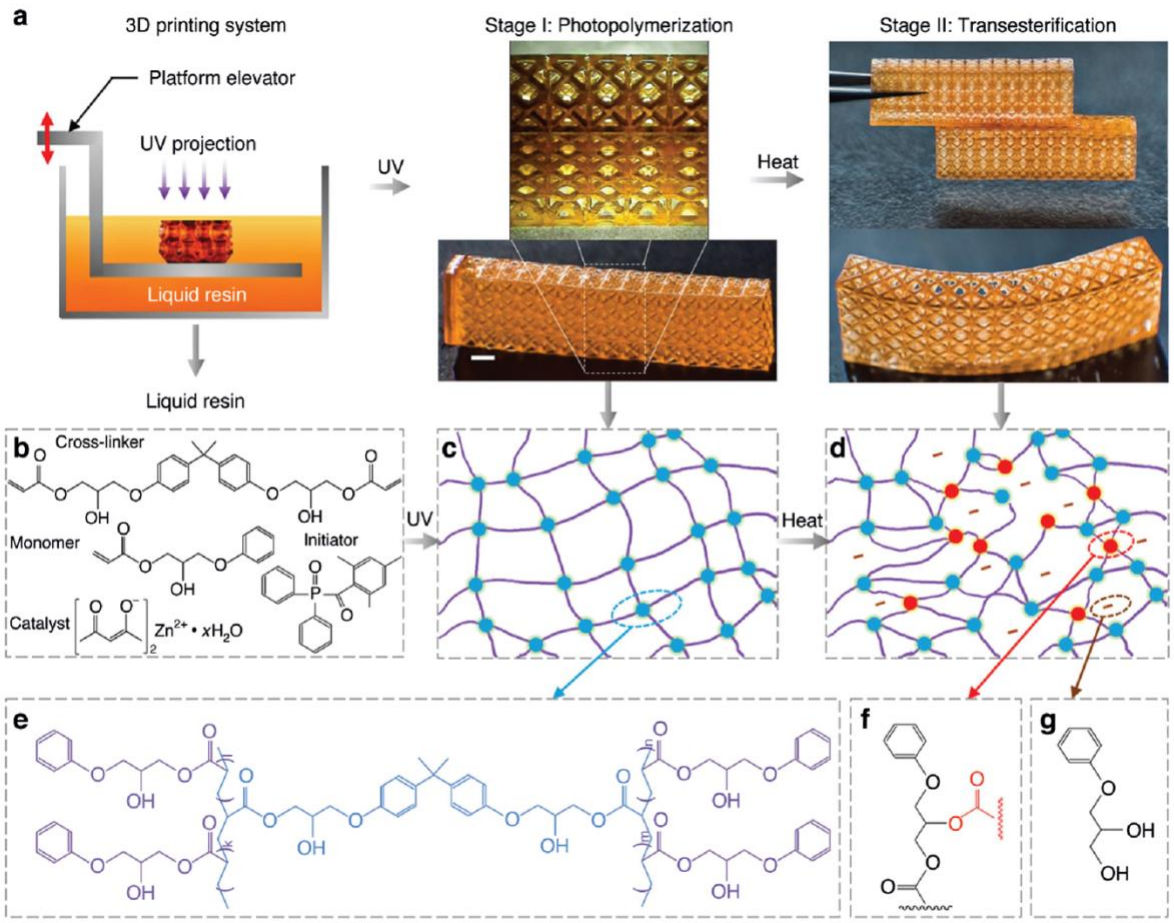

Figure 24: (a) Schematic depicting the complete process of 3D printing and photopolymerization to transesterification for reprocessing. (b) Monomers in the liquid resin. (c) Illustration of the network. (d) Illustration of transesterification. (e) Chemical structure of network, (f) and (g) Chemical structures from the transesterification rearrangement.[80] Reproduced from Ref. 80 under the terms of the Creative Commons CC BY license (https://creativecommons.org/licenses/by/4.0/), copyright © 2018, Zhang et al., published by Springer Nature, no changes were made.

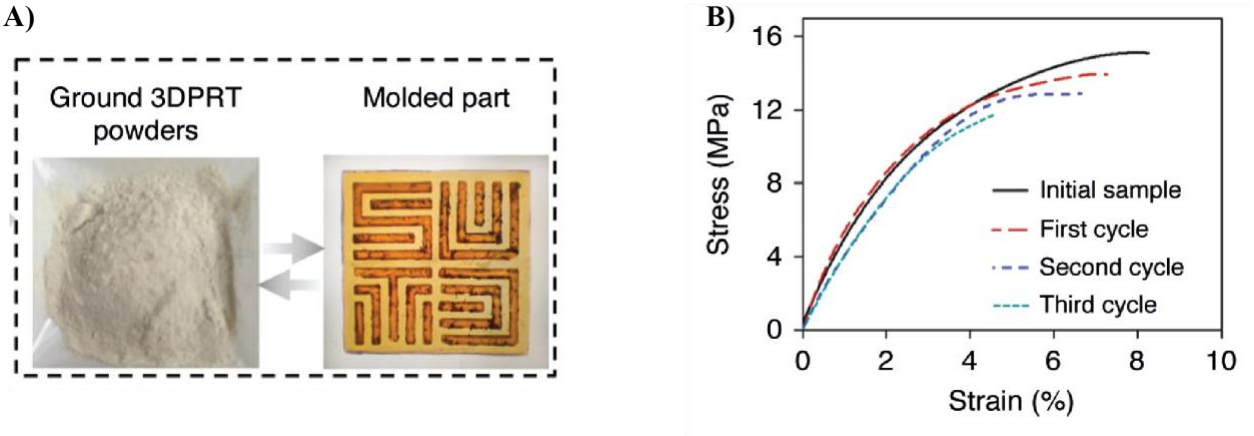

Figure 25: A) Image depicting a ground 3D printed part and the remolded part enabled by transesterification.[80] **B)** Tensile stress vs strain measurements of reprocessed samples over three recycling rounds.[80] Reproduced from Ref. 80 under the terms of the Creative Commons CC BY license (https://creativecommons.org/licenses/by/4.0/), copyright © 2018, Zhang et al., published by Springer Nature, no changes were made.

Diels-Alder linkages have also been utilized to allow for reprocessing. Diels-Alder linkages between a furan and maleimide group were formed within a di-acrylate crosslinker, then incorporated into the monomer formulation on its own, or with HEA as a co-monomer.[81] The dynamic reversibility of the Diels-Alder bond allows for networks to be de-crosslinked upon heating and then re-crosslinked upon cooling. Li *et.al.* demonstrated that the recycling efficiency of these networks was between 54% and 69% by comparing the reprocessed properties to those of

the original sample, indicating that the tensile strength and elongation at break decrease slightly during the recycling process.[81]

Overall, these studies demonstrate successful 3D printing of CANs and their subsequent thermal reprocessing to form other parts, a process that can help reduce the plastic waste compared to traditional 3D printed thermosets. Additional research is needed to better understand the possibilities for 3D printed CANs and this will be discussed further in section 3.2.

2.2 Degradable Materials

Another important sustainable end-of-life pathway for 3D printed materials is degradation post use. 3D printed parts that contain degradable moieties are an attractive alternative to conventional SLA/DLP thermosets as these can mitigate the accumulation and cost of waste management. Degradable thermosets can incorporate recovery and reuse of starting materials, diverse degradation behavior depending on the type of degradable linkage, different types of degradation triggers suitable for end applications, and recovery of high-value components from thermoset composites.[82] A very common mode of thermoset degradation is chain cleavage through abiotic (non-enzymatic) hydrolysis or enzymatic hydrolysis.[83] Environmental biodegradation of thermosets through microorganisms is also encountered in natural environments such as soil and marine water.[83] This section will provide an overview of studies that have incorporated degradable linkages in 3D printed networks. For a list of these studies please see Table 1. Most of the articles described in this section focus on 3D printed parts intended for *in-vivo* biomedical applications. For such applications, degradation after service life is more important than reprocessing since the material will potentially remain *in-vivo* after end-of-life and cannot be taken out. In some studies, the toxicity of degradation products is also considered since cytotoxicity is crucial in biomedical applications.

To make 3D printing formulations degradable, one strategy has been to synthesize photopolymerizable macromers from existing synthetic polyesters or polycarbonates. Such degradable and UV curable resins have been commonly derived from PLA,[39,84] poly(trimethylene carbonate) (PTMC),[33,85] poly(propylene fumarate) (PPF),[86] PCL,[33,35,39] and poly(glycerol sebacate) (PGS).[35] With the exception of PPF, which contains one carbon-carbon double bond per repeat unit, all other synthetic polyesters or polycarbonates have been functionalized with acrylate groups to allow for photopolymerization.

SLA has been used to fabricate hydrogel structures from PEG for application as tissue engineering scaffolds.[35] To impart degradability to these hydrogel structures, a common strategy has been to synthesize block copolymer macromers from PEG and polyesters. Seck *et.al.* synthesized PDLLA-PEG-PDLLA triblock copolymers, which were end capped with methacrylate groups to obtain crosslinkable macromers (Figure 26A).[84] SLA printed PDLLA-PEG hydrogel structures (Figure 26B) underwent rapid degradation within 5 seconds when immersed in 1 M NaOH solution, leaving behind a clear PEG solution.[84] This rapid degradation was due to the hydrolytically labile ester bonds in the PDLLA blocks. A similar strategy was employed by Sharifi *et.al.* to develop degradable hydrogels based on PTMC-PEG-PTMC triblock copolymers end-capped with methacrylate groups.[85] The PTMC-PEG hydrogels were shown to be enzymatically degradable by porcine pancreatic cholesterol esterase due to the ester bonds in the PTMC blocks.[85] After 5 weeks of incubation in enzyme containing media, PTMC-PEG hydrogels with a PTMC block length of 5 kDa underwent almost complete degradation with a mass loss of 84%.[85] This enzymatic degradation is important since these materials are intended for medicinal and tissue engineering applications.

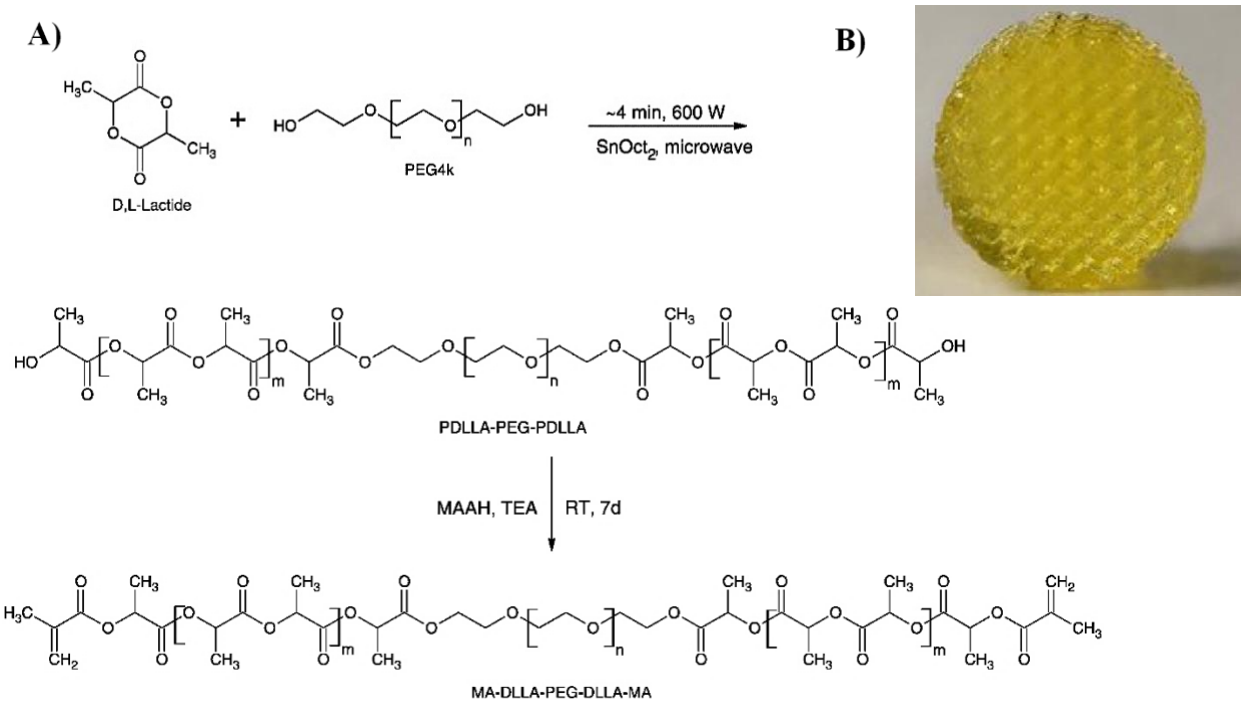

Figure 26: A) Synthesis of PDLLA-PEG-PDLLA triblock copolymers, followed by end functionalization with methacrylic anhydride (MAAH) to install methacrylate groups.[84] **B)** Photograph of hydrogel scaffold with gyroid pore network. The diameter of hydrogel disk is 8 mm.[84] Reprinted from *J. Control. Release*, 148, T. M. Seck, F. P. W. Melchels, J. Feijen, D. W. Grijpma, Designed biodegradable hydrogel structures prepared by stereolithography using poly(ethylene glycol)/poly(d,l-lactide)-based resins, 34–41, Copyright (2010), with permission from Elsevier.

SLA has also been used to develop hydrolysable tissue engineering scaffolds from homopolymers containing ester bonds instead of block copolymers. For instance, Walker *et.al.* utilized only PPF for the development of scaffolds.[86] In this study, PPF was synthesized by ring-opening copolymerization of propylene oxide and maleic anhydride (Figure 27A). The carbon-carbon double bond in the PPF backbone allows for printing without any further synthetic modifications when mixed with a reactive diluent. The printed PPF scaffolds could be readily degraded in 0.1 M NaOH solution due to the ester linkages in the polymer backbone. The

degradation rate of these thermosets could be tuned with polymer molecular weight and scaffold pore architecture (coarse vs fine), as depicted by the mass loss data in Figure 27B, and optical micrographs of degraded scaffolds in Figure 27C.[86] Additionally, the degradation products of PPF hydrolysis are non-toxic propylene glycol and fumaric acid, which is attractive from the point of view of printed parts that may end up in the environment and degrade.[86]

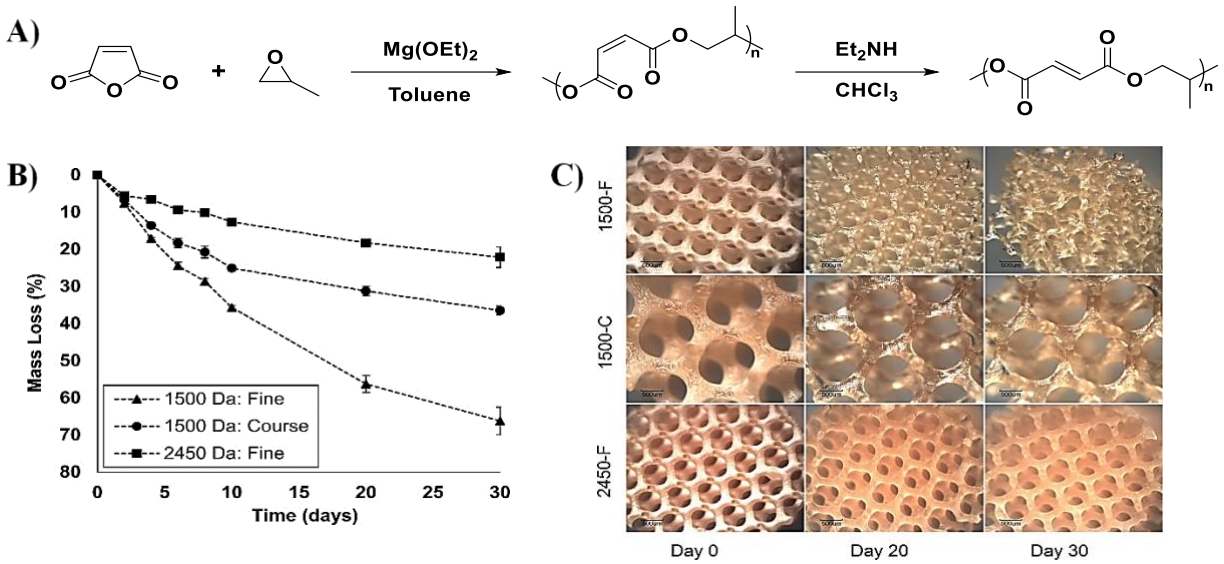

Figure 27: A) Synthesis of PPF.[87] **B)** Mass loss of PPF scaffolds during degradation tests demonstrating the effect of PPF molecular weight and scaffold pore architecture (course vs fine).[86] **C)** Optical micrographs of PPF scaffolds degraded in 0.1M NaOH. It is shown that after 30 days, scaffolds with PPF molecular weight of 1500 Da and a fine pore architecture are the most heavily degraded (top part of the image, 1500-F).[86] Panels A reprinted with permission from { Y. Luo, C. K. Dolder, J. M. Walker, R. Mishra, D. Dean and M. L. Becker, Synthesis and Biological Evaluation of Well-Defined Poly(propylene fumarate) Oligomers and Their Use in 3D Printed Scaffolds, *Biomacromolecules*, 2016, **17**, 690–697. https://pubs.acs.org/doi/abs/10.1021/acs.biomac.6b00014} Copyright {2016} American Chemical Society. Further permissions related to the material excerpted should be directed to ACS. Panels B and C reprinted with permission from {J. M. Walker, E. Bodamer, O. Krebs, Y. Luo, A.

Kleinfehn, M. L. Becker and D. Dean, Effect of Chemical and Physical Properties on the In Vitro Degradation of 3D Printed High Resolution Poly(propylene fumarate) Scaffolds, *Biomacromolecules*, 2017, **18**, 1419–1425} Copyright {2017} American Chemical Society.

Degradable 3D printing networks have also been developed by copolymerization of different cyclic ester and carbonate monomers leading to networks with tunable degradation properties depending on the ratio of the different comonomers. Kuhnt *et.al.* took advantage of the difference in sensitivity towards hydrolytic degradation of CL and TMC, and fabricated scaffolds based on CL and TMC.[33] In this study, poly(CL-*co*-TMC) random copolymers were synthesized with varying CL:TMC ratios, and the copolymers were end-capped with acrylate groups to create networks (Figure 28A). By varying the CL:TMC ratio in the copolymer, the thermal and mechanical properties of the crosslinked networks could be modulated over a wide range as shown in Figure 28B-C. Interestingly, these CL/TMC networks underwent hydrolytic degradation when immersed in 0.1 M NaOH solution at 37 ℃. A range of degradation rates could be obtained by changing the ratio of CL to TMC as shown in Figure 28D. In general, a higher TMC content in the copolymer lead to a slower degradation rate.[33] This study also demonstrated successful DLP printing of the 25:75 CL:TMC resin to fabricate scaffolds with gyroid structure as shown in the optical microscopy and SEM images in Figure 28E. A similar strategy was employed by Felfel *et.al.* that developed degradable scaffolds from methacrylated random copolymers of LA and CL.[39] In this study, LA and CL were copolymerized, followed by end-functionalization to create di-methacrylated random PLA-PCL copolymers with varying LA to CL ratios (Figure 29).[39] The T_g, compressive modulus, and compressive strength of the SLA crosslinked scaffolds could be tuned over the range of 4.8 ℃ to 33 ℃, 0.26 MPa to 4.14 MPa, and 0.05 MPa to 0.56 MPa, respectively, by increasing the LA:CL ratio. Hydrolytic degradation of the PLA-PCL networks was evaluated

by immersing them in PBS solutions of pH 7.4 at varying temperatures. The results indicated that at any given degradation temperature, the degradation rate could be increased by increasing LA content in the copolymer.[39] For instance, scaffolds with a LA:CL ratio of 18:2 underwent 68% mass loss in 39 days at 50 °C, whereas those with LA:CL ratio of 16:4 had a mass loss of 41.5% under the same conditions.[39] In another study by Chen *et.al.*, degradable networks were created by combining three different types of acrylated prepolymers based on PEG, PCL, and PGS as discussed in the Polyesters section.[35] Hydrolytic degradation of these networks due to ester bonds was evaluated in the presence of an enzyme lipase. The degradation rate was faster for networks with higher PGS content, due to the fact that the PGS backbone contains the highest number of polyester linkages in the network.[35]

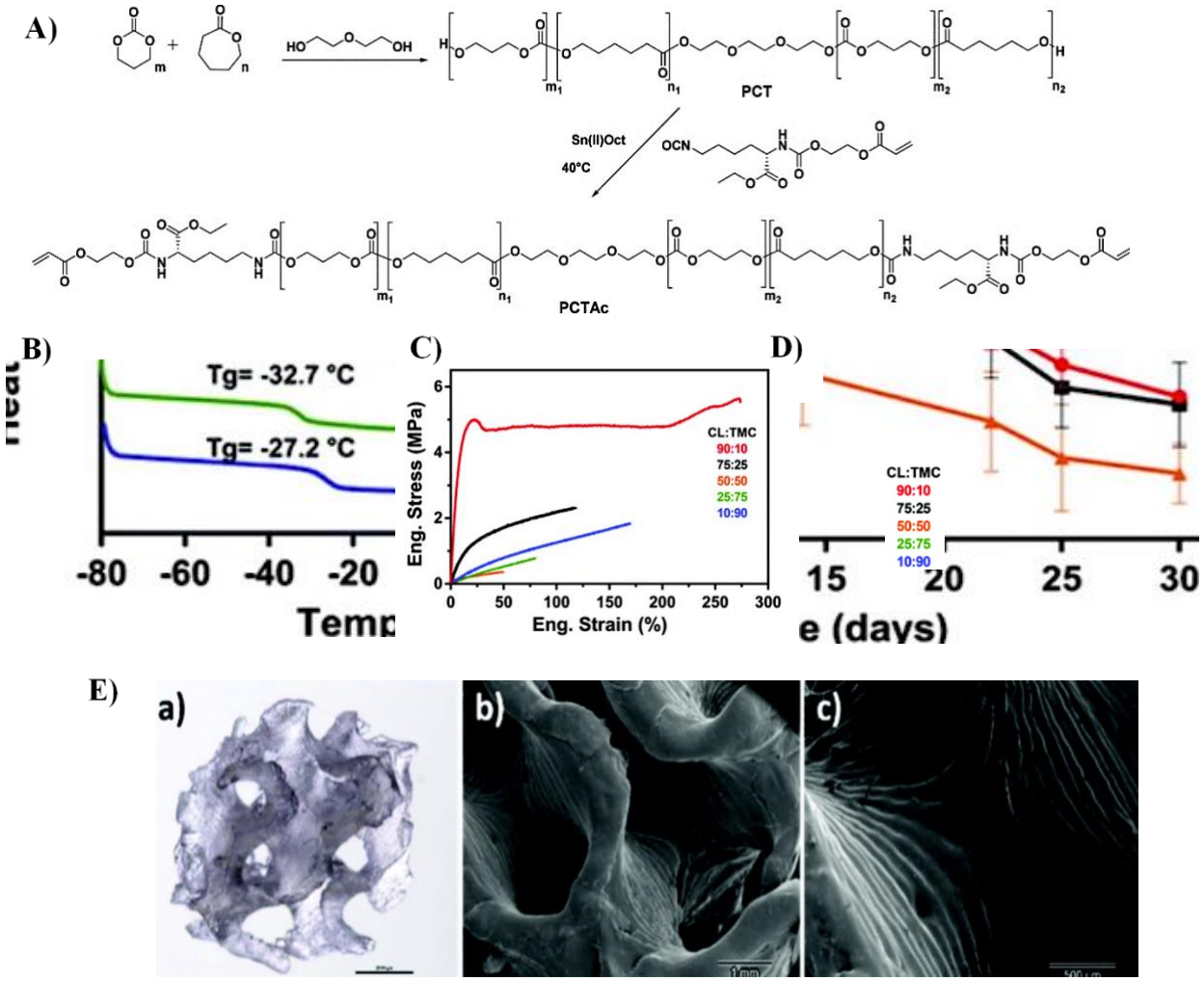

Figure 28*:* A) Synthesis of poly(CL-*co*-TMC) random copolymers followed by acrylate end group functionalization.[33] **B)** DSC traces, and **C)** Engineering stress-strain curves of thermoset films.[33] **D)** Mass loss over time of CL:TMC copolymer networks when immersed in 0.1 M NaOH.[33] **E)** Optical microscopy (a) and SEM images (b, c) of the fabricated gyroid scaffold. The third image (c) is an SEM zoom-in showing the different printing layers. Scale bars are 1 mm and 500 μm, respectively.[33] Reproduced from Ref. 33 with permission from the Royal Society of Chemistry.

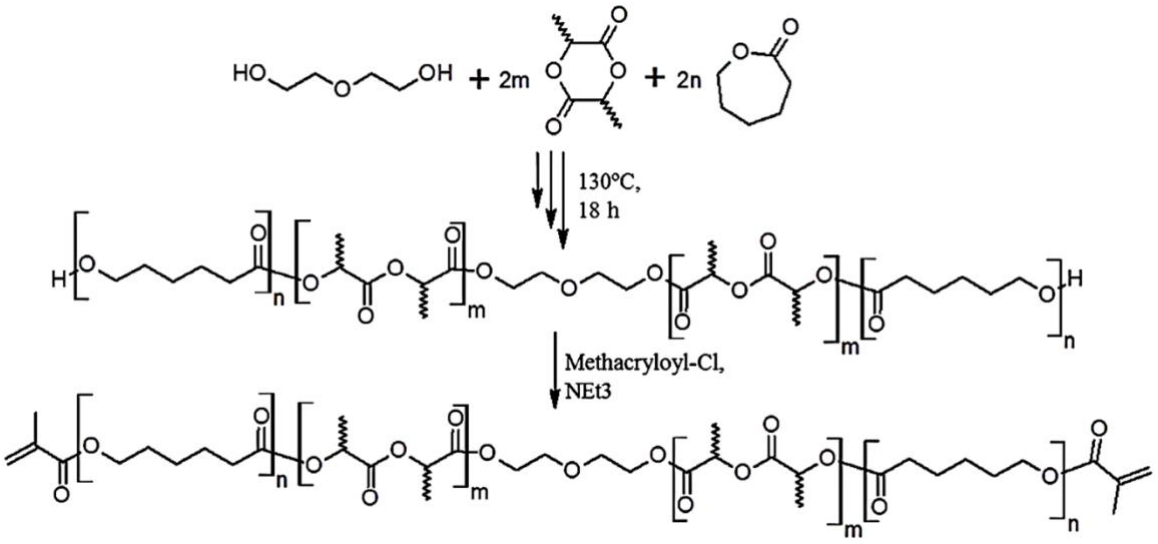

Figure 29: Synthesis of PLA-PCL random copolymers followed by methacrylation.[39] Reproduced from R. M. Felfel, L. Poocza, M. Gimeno-Fabra, T. Milde, G. Hildebrand, I. Ahmed, C. Scotchford, V. Sottile, D. M. Grant and K. Liefeith, In vitro degradation and mechanical properties of PLA-PCL copolymer unit cell scaffolds generated by two-photon polymerization, *Biomed. Mater.*, 11, 015011, 1st December 2015, DOI: 10.1088/1748-6041/11/1/015011. Copyright © IOP Publishing. Reproduced with permission. All rights reserved.

Apart from synthetically modifying existing polyesters to make degradable systems, a second strategy has been to develop other distinct monomers and polymers that contain degradable linkages. These monomers or polymers utilize the hydrolytic sensitivity of ester,[29,34,88] and carbonate linkages,[89] and the enzymatic sensitivity of proteins to make the 3D printed parts degradable.[71,90] Sirrine *et.al.* took advantage of the hydrolytic sensitivity of ester bonds, and synthesized poly(tri(ethylene glycol) adipate) di-methacrylate resin via melt polycondensation of tri(ethylene glycol) and adipic acid (Figure 30A).[88] The resulting SLA-printed thermoset underwent hydrolytic degradation due to ester bonds when immersed in concentrated hydrochloric acid solution for a period of 4 hours.[88] This short time-scale degradation was monitored via SEM, where surface degradation and cracking could be observed (Figure 30B-C).[88]

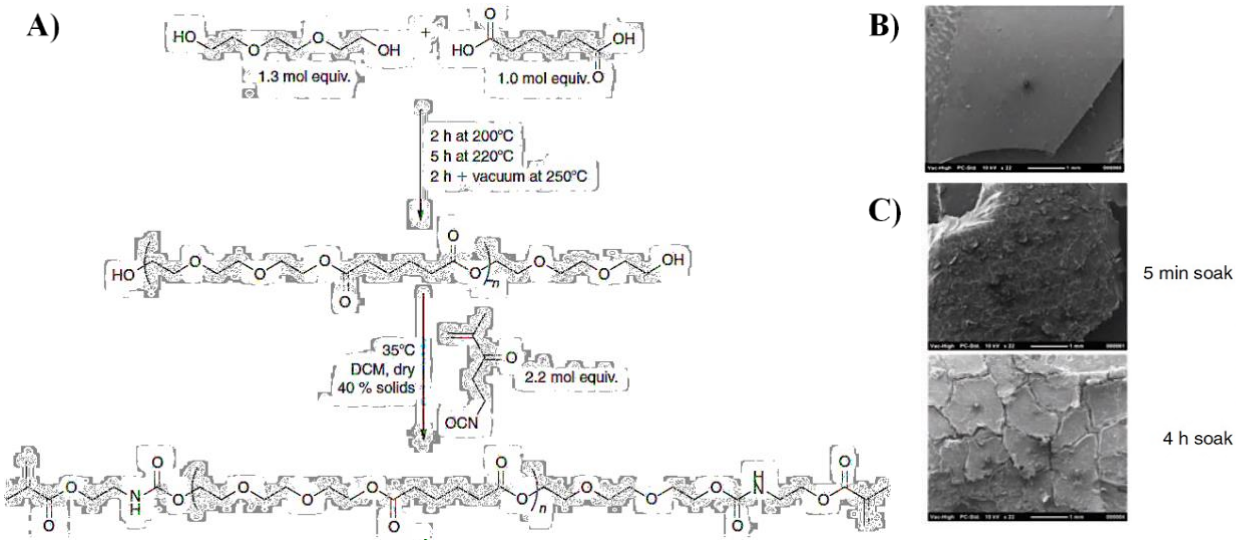

Figure 30: A) Synthesis of poly(tri(ethylene glycol) adipate) di-methacrylate resin.[88] **B)** SEM micrograph of neat polyester film, and **C)** SEM micrograph of polyester film treated with concentrated HCl, indicating hydrolysis induced surface cracking.[88] Republished with permission of CSIRO Publishing from J. M. Sirrine, A. M. Pekkanen, A. M. Nelson, N. A. Chartrain, C. B. Williams and T. E. Long, 3D-Printable Biodegradable Polyester Tissue Scaffolds for Cell Adhesion, *Aust. J. Chem*., 68, 2015; permission conveyed through Copyright Clearance Center, Inc.

Carbonate linkages have also been incorporated in 3D printing to impart degradability. Oesterreicher *et.al.* synthesized 6 novel terminal alkyne carbonate monomers (Figure 31A) and crosslinked them with commercially available multifunctional thiols (Figure 31B) to create thermosets.[89] Hydrolytic degradability of these networks due to the carbonate linkages in the alkyne monomers, and ester linkages in the thiol crosslinkers, was studied by immersing them in 1M NaOH or 1M HCl solution at 45 °C. The degradation rate was faster under basic conditions, and could be selectively tuned by the choice of alkyne and thiol monomers (Figure 31C).[89]

Degradation results under basic conditions were further extrapolated to estimate full degradation time of the different thermosets, which ranged from a week to a month depending on the monomer and crosslinker chosen.[89] An additional benefit of this step-growth thiol-alkyne system from the point of view of sustainability is that the degradation products are low molecular weight fragments. This is in contrast with chain-growth acrylate systems, in which high molecular weight polyacrylate chains are formed as degradation products. This study also demonstrated successful DLP printing of the TCBC/DiPETMP alkyne-thiol combination with an accuracy of 40×40 µm as shown in Figure 31D.

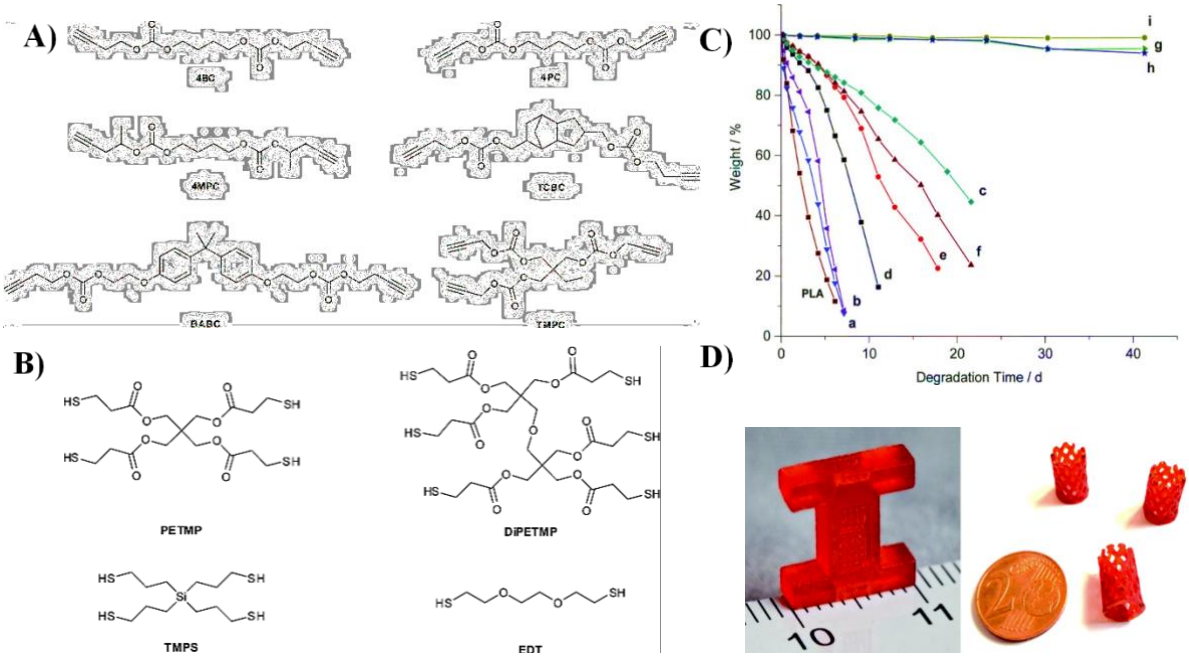

Figure 31: A) Synthesized alkyne-carbonate monomers.[89] **B)** Thiols used in photopolymerization.[89] **C)** Weight loss of alkyne-thiol thermosets in 1M NaOH (a) 4PC/PETMP, (b) 4BC/PETMP, (c) 4MPC/PETMP, (d) 4PC/5TMPS, (e) 4PC/10TMPS, (f) 4PC/20TMPS, (g) 4PC/EDT, (h) BC/EDT, (i) MPC/EDT, and control PLA.[89] **D)** DLP printed patterns from TCBC/DiPETMP formulation.[89] Reproduced from Ref. 89 with permission from the Royal Society of Chemistry.

Along with hydrolytically sensitive linkages, enzymatic sensitivity of proteins has also been exploited to introduce biodegradability in 3D printing formulations.[71,90] Gelatin, which is a protein, has been used to create degradable 3D printing compositions. Wang *et.al.* reacted the lysine units of gelatin with methacrylic anhydride to synthesize gelatin methacryloyl (GelMA).[90] GelMA was mixed with PEGDA and a water-soluble photoinitiator to 3D print helical microstructures via two photon polymerization (Figure 32A). These microstructures could be used as small-scale biodegradable robots for applications such as cell adhesion and growth.[90] Enzymatic degradation of GelMA microstructures was evaluated by immersing them in PBS solutions containing the enzyme collagenase at different concentrations (0.01 mg mL^{-1} to 0.5 mg mL^{-1}).[90] Collagenase cleaves the amide bonds of the peptide domains in gelatin leading to degradation of the GelMA microstructures (Figure 32B). The degradation studies revealed that the GelMA degradation time (the time required for the GelMA microstructures to completely disappear), could be easily tuned from nearly 130 seconds to 48 mins by varying the enzyme concentration and the swimmer shape and dimensions (Figure 32C).[90]

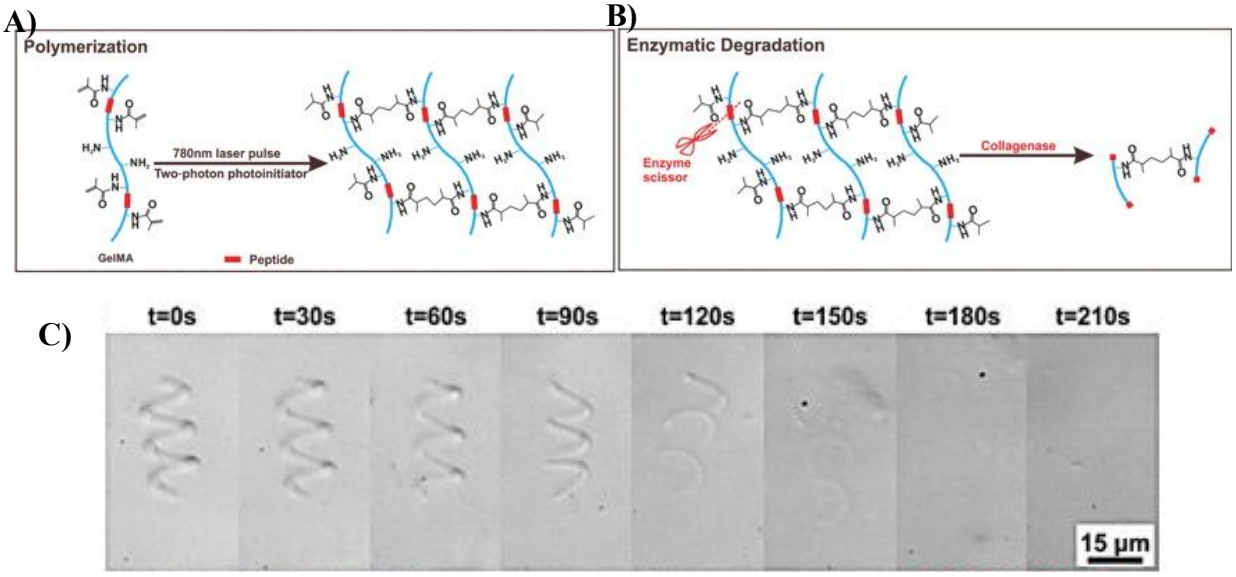

Figure 32: A) Schematic depicting polymerization, and **B)** enzymatic degradation mechanism of GelMA.[90] **C)** Degradation of GelMA microswimmers in collagenase solution of 0.1 mg mL^{-1}.[90] Reprinted with permission from X. Wang, X. H. Qin, C. Hu, A. Terzopoulou, X. Z. Chen, T. Y. Huang, K. Maniura-Weber, S. Pané and B. J. Nelson, 3D Printed Enzymatically Biodegradable Soft Helical Microswimmers, *Adv. Funct. Mater.*, 2018, **28**, 1–8. Copyright © 2018 WILEY-VCH Verlag GmbH & Co. KGaA, Weinheim.

Overall, the studies described in this section demonstrate that two different strategies have been utilized to render 3D printed parts degradable. In the first strategy, existing synthetic polyesters/polycarbonates are modified to introduce acrylate or methacrylate end groups for UV crosslinking. The resulting SLA/DLP fabricated thermosets are susceptible to hydrolytic degradation due to the ester/carbonate linkages in the polymer backbone. A range of studies that implement this strategy on PLA, PCL, PPF, PTMC, and PGS platforms have been discussed. In some studies, 3D printable copolymers have been synthesized using different ester/carbonate monomers to obtain thermosets with tunable degradation rates based on comonomer ratios. In the second strategy other distinct monomers or polymers containing hydrolytically sensitive ester and carbonate linkages or enzymatically sensitive proteins, such as gelatin and BSA (discussed in section 1.1.3), have been developed. However, as mentioned previously, all the studies described in this section focus on 3D printed materials intended for *in vivo* biomedical applications, which do not contribute to environmental plastic waste. Hence, implementation of these strategies in formulations directed towards non-biomedical 3D printing applications is crucial, as it will ultimately aid in reducing environmental 3D printed plastic waste by making these parts degradable after end-of-life. For instance, 3D printing formulations to be used predominantly for prototyping applications could incorporate more degradable chemistry such as PLA/PGS

platforms discussed in this section. This will enable prototypes, which have a shorter lifetime than manufacturing/biomedical materials, to be rapidly degraded through ester hydrolysis after printing, thereby preventing their contribution to plastic waste.

3. Future Perspectives

So far, current research progress in the design of sustainable SLA/DLP formulations has been presented considering the Feedstock (Sections 1.1 Renewable and 1.2 Waste) and the End-Of-Use (Sections 2.1 Reprocessable and 2.2 Degradable).[9] In this third section, we will briefly summarize some aspects of sustainability that have not yet been incorporated in SLA/DLP resins. These could serve as possible future research directions in the field of sustainable 3D printing.

3.1 Recycling: Feedstock and End-Of-Use

Recycling is a very important step in creating sustainable materials and reducing the waste produced from SLA/DLP parts. The two sections that have been identified as needing more attention within the SLA/DLP 3D printing industry are: Recycled Feedstock and End-Of-Use Chemical Recycling. Recycled feedstock applies, in this specific case, to a resin that can be 3D printed and recycled for direct reuse in 3D printing. One example of chemistry that would allow for feedstock recycling is based on thiol-thioester exchange (a mechanism similar to transesterification).[91] Thiol-thioester exchange allows for the regeneration of thiol groups after photopolymerization upon addition of excess thiol crosslinker and base.[91] The regenerated thiol groups can be reacted with allyl or acrylate monomers used in the original resin via thiol-ene chemistry to generate new 3D printed parts (Figure 33).[91] However, this is only one example of feedstock recycling that could be applied to SLA/DLP and more research focused on SLA/DLP feedstock recycling is necessary.

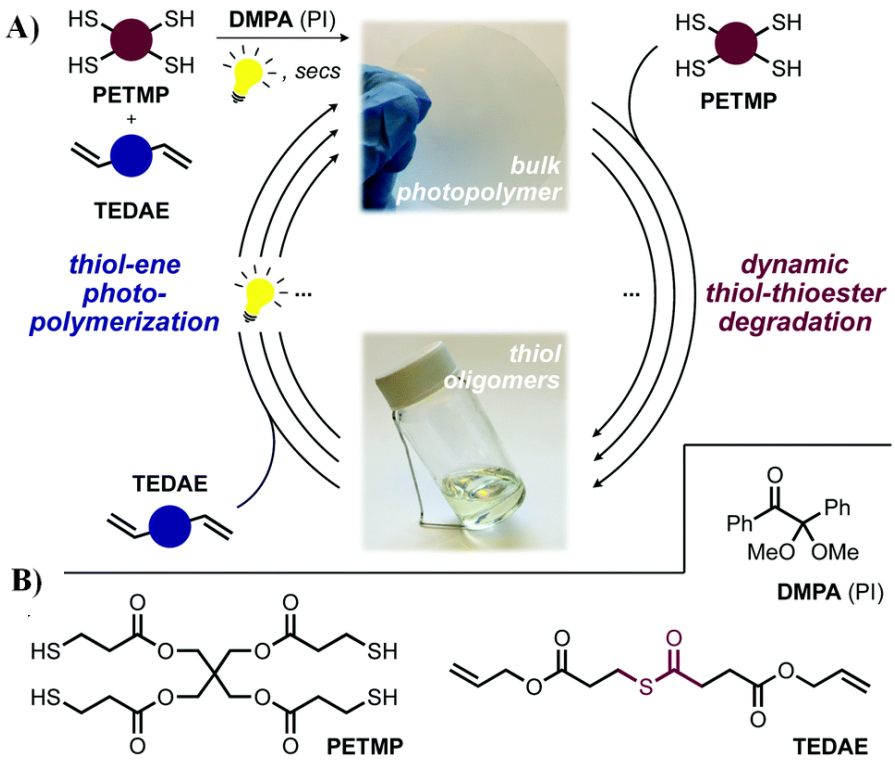

Figure 33: A) Feedstock recycling based on thiol-thioester exchange mechanism, and **B)** chemical structures of monomers and photoinitiator.[91] Reproduced from Ref. 91 with permission from the Royal Society of Chemistry.

The second section that has been identified for future research directions is chemical recycling as an end-of-use method. Chemical recycling involves the use of chemical or thermal processes to depolymerize 3D printed parts into smaller fragments or starting monomers. These fragments or monomers can be utilized as raw materials in the same 3D printing process, or as feedstock for other processes/applications.[92] Chemical recycling provides an efficient route to reduce both plastic waste and economic losses,[92] however, it seems to be an overlooked area of research in SLA/DLP 3D printing and should be the focus of future studies.

3.2 Reprocessable: End-of-Use

Reprocessing as an end-of-use method focuses on reusing printed material in applications other than printing, for example remolding, thereby reducing SLA/DLP plastic waste. While two

categories of reprocessing have been discussed in section 2.1, a vast amount of chemistry has been developed that could be utilized to improve the reprocessability of 3D printed parts. One such example is the chemistry of SLA/DLP self-healing materials, which typically only demonstrate repairability, but could be further adapted for reprocessing. One example of SLA/DLP self-healing materials that could be used for reprocessing utilizes disulfide bonds.[93] Li *et.al.* showed that materials containing disulfide bonds could be healed at 80 °C for 12 hrs at least three times with minimal loss in tensile properties (Figure 34).[93] SLA/DLP materials could theoretically be remolded at this temperature and hence reprocessed. Evaluation of reprocessable materials within SLA/DLP 3D printing should be expanded, and a good starting point could be to look at existing self-healing chemistries and assessing their potential use for reprocessing.

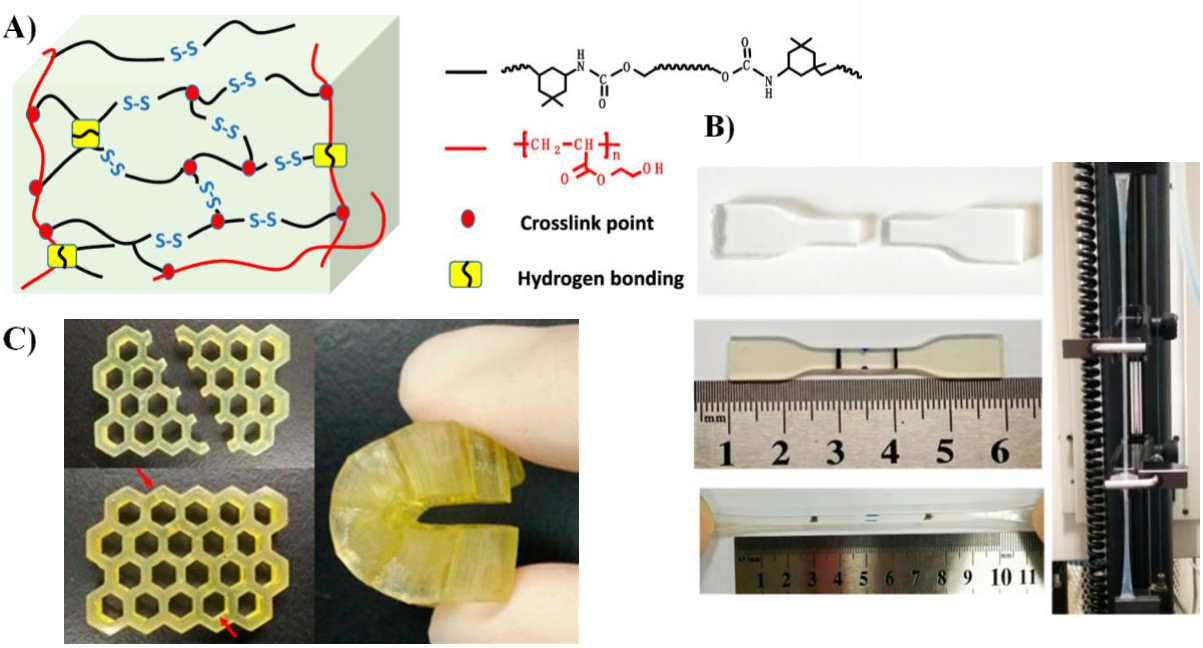

Figure 34: A) Schematic depicting the synthetic strategy of disulfide bonds based self-healing materials.[93] **B)** Images depicting self-healing of tensile test specimens. The specimens are cut into two parts, healed at 80 °C for 12 hrs, and then stretched to a large deformation.[93] **C)** Self-healing of the DLP printed honeycomb structure. The honeycomb structure was cut into two parts, healed at 80 °C for 12 hrs, and then could be freely bent.[93] Reprinted with permission from {X. Li, R. Yu,

Y. He, Y. Zhang, X. Yang, X. Zhao and W. Huang, Self-Healing Polyurethane Elastomers Based on a Disulfide Bond by Digital Light Processing 3D Printing, *ACS Macro Lett*., 2019, 8, 1511–1516, https://pubs.acs.org/doi/10.1021/acsmacrolett.9b00766} Copyright {2019} American Chemical Society. Further permissions related to the material excerpted should be directed to ACS.

3.3 Biodegradation: End-of-Use

Although hydrolytic degradation of 3D printed parts has been widely studied in SLA/DLP, microorganism mediated biodegradation has been a focus of only a handful of studies. One example of this is the study utilizing McDonald's waste cooking oil discussed in Section 1.2.[75] This study demonstrated microbial degradation of waste cooking-oil thermosets by soil burial tests.[75] It is essential that future studies incorporate different biodegradable linkages within their resin to facilitate the biodegradation of 3D printed parts in natural environments such as, marine water, fresh water, or soil, since these parts can leak into the environment after use. Identification and evaluation of biodegradation products is also essential to prevent further harm to animals and the environment. Future studies can also work on exploring different degradable linkages other than ester linkages in SLA/DLP compositions, some examples of which include acetal/hemiacetal, carbonate, orthoester, carbamate, and disulfide linkages (different degradable linkages for thermosets have been reviewed recently).[82] Use of different types of degradable linkages can offer a diverse range of degradation behavior in 3D printed parts, along with different types of degradation triggers suitable for both the desired application and end-of-use environment.

Conclusions

The 3D printing market has experienced an annual growth rate of 10% in the past few years, and this rapid growth is expected to continue.[2,3] However, along with the rapid growth, comes an alarming increase in the amount of plastic waste produced by the 3D printing industry.

Particularly, SLA/DLP 3D printed products are generally petroleum-based thermosets that are contributing to plastic waste and further aggravating the worsening plastic pollution problem. It is crucial to mitigate the production and accumulation of 3D printing plastic waste, and this can be achieved by developing more sustainable alternatives. This review serves as an overview of many of the sustainable advances in SLA/DLP 3D printing to date and it describes their entire lifetime, from feedstock selection to monomer preparation to end-of-life.[9] Additionally, special attention is placed on research that has employed green chemistry principles in their syntheses and those demonstrating sustainable 3D printed parts that have properties comparable to petroleum-based materials. Overall, this review shows that extensive research is currently being undertaken to transform SLA/DLP processes and materials into more sustainable versions. Efforts directed towards feedstock, end-of-life, green synthetic procedures, and competitive material properties relative to petroleum-based products are all part of the sustainability strategy. However, this review also highlights that many other aspects of sustainability, such as recycling for feedstock/end-of-use and biodegradation of 3D printed parts in natural environments, have not yet been explored in SLA/DLP and could serve as opportunities for future research. It is clear that the future is bright for 3D printing and there are ample opportunities for chemists and engineers alike to have an impact in further sustainability developments in this area.

Acknowledgements

We acknowledge our funding sources for this work, the NSF Center for Sustainable Polymers at the University of Minnesota, a National Science Foundation supported Center for Chemical Innovation (CHE-1901635) and the National Science Foundation Graduate Research Fellowship Program (to E. M. Maines) under grant no. CON-75851, project 00074041. Any opinions, findings, and conclusions or recommendations expressed in this material are those of the

author(s) and do not necessarily reflect the views of the National Science Foundation. The authors acknowledge the Sustainable Polymer Framework developed by the NSF Center for Sustainable Polymers at the University of Minnesota that provided insight for the layout of this article.

References

1 A. H. Tullo, 3-D printing firms rise to coronavirus challenge, https://cen.acs.org/materials/3-d-printing/3-D-printing-firms-rise/98/web/2020/03, (accessed 16 November 2020).

2 D. Stewart, Technology, Media, and Telecommunications Predictions 2019: 3D printing growth accelerates again, https://www2.deloitte.com/content/dam/insights/us/articles/TMT-Predictions_2019/DI_TMT-predictions_2019.pdf, (accessed 5 October 2020).

3 S. Karevska, G. Steinberg, A. Müller, R. Wienken, C. Kilger and D. Krauss, 3D printing: hype or game changer?, https://assets.ey.com/content/dam/ey-sites/ey-com/en_gl/topics/advisory/ey-3d-printing-game-changer.pdf, (accessed 21 October 2020).

4 D. Lipodio, V. Colombi, G. D'Alessandro and C. Verdiana, The Future of Health Care. Potential, impact and models of 3D printing in the Health Care sector, https://www2.deloitte.com/content/dam/Deloitte/be/Documents/life-sciences-health-care/The future of Health Care_ENG.pdf, (accessed 21 October 2020).

5 R. Geyer, in *Plastic Waste and Recycling*, ed. T. M. Letcher, Academic Press, 2020, pp. 13–32.

6 R. E. Drumright, P. R. Gruber and D. E. Henton, Polylactic Acid Technology, *Adv. Mater.*, 2000, **12**, 1841–1846.

7 4,929,402, 1990, 1–13.

8 V. S. D. Voet, J. Guit and K. Loos, Sustainable Photopolymers in 3D Printing: A Review on Biobased, Biodegradable, and Recyclable Alternatives, *Macromol. Rapid Commun.*, 2020, **2000475**, 1–11.

9 J. E. Wissinger, C. J. Ellison, W. R. Dichtel, J. T. Trotta, A. B. Chang, A. Yang and C. W. Bunyard, *Sustainable Polymer Framework*, 2020.

10 P. Anastas and N. Eghbali, Green chemistry: Principles and practice, *Chem. Soc. Rev.*, 2010, **39**, 301–312.

11 A. D. Curzons, D. J. C. Constable, D. N. Mortimer and V. L. Cunningham, So you think your process is green, how do you know? - Using principles of sustainability to determine

what is green - A corporate perspective, *Green Chem.*, 2001, **3**, 1–6.

12 Avantor, Diphenyl(2,4,6-trimethylbenzoyl)phosphine Oxide Safety Data Sheet, https://us.vwr.com/assetsvc/asset/en_US/id/16490607/contents, (accessed 18 February 2020).

13 ECHA, Diphenyl(2,4,6-trimethylbenzoyl)phosphine oxide, https://echa.europa.eu/brief-profile/-/briefprofile/100.071.211, (accessed 17 February 2020).

14 W. D. Callister and D. G. Rethwisch, *Materials Science and Engineering an Introduction*, John Wiley & Sons, Inc., 4th edn., 2012.

15 Formlabs, Material Data Sheet Standard, https://formlabs-media.formlabs.com/datasheets/Standard-DataSheet.pdf, (accessed 18 February 2020).

16 C.-H. Zhou, X. Xia, C.-X. Lin, D.-S. Tong and J. Beltramini, Catalytic conversion of lignocellulosic biomass to fine chemicals and fuels, *Chem. Soc. Rev.*, 2011, **40**, 5588.

17 F. H. Isikgor and C. R. Becer, Lignocellulosic biomass: a sustainable platform for the production of bio-based chemicals and polymers, *Polym. Chem.*, 2015, **6**, 4497–4559.

18 R. Singh, A. Shukla, S. Tiwari and M. Srivastava, A review on delignification of lignocellulosic biomass for enhancement of ethanol production potential, *Renew. Sustain. Energy Rev.*, 2014, **32**, 713–728.

19 L. Pezzana, E. Malmström, M. Johansson and M. Sangermano, UV-Curable Bio-Based Polymers Derived from Industrial Pulp and Paper Processes, *Polymers (Basel).*, 2021, **13**, 1530.

20 J. T. Sutton, K. Rajan, D. P. Harper and S. C. Chmely, Lignin-Containing Photoactive Resins for 3D Printing by Stereolithography, *ACS Appl. Mater. Interfaces*, 2018, **10**, 36456–36463.

21 R. Ding, Y. Du, R. B. Goncalves, L. F. Francis and T. M. Reineke, Sustainable near UV-curable acrylates based on natural phenolics for stereolithography 3D printing, *Polym. Chem.*, 2019, **10**, 1067–1077.

22 A. W. Bassett, A. E. Honnig, C. M. Breyta, I. C. Dunn, J. J. La Scala and J. F. Stanzione, Vanillin-Based Resin for Additive Manufacturing, *ACS Sustain. Chem. Eng.*, 2020, **8**, 5626–5635.

23 A. Navaruckiene, E. Skliutas, S. Kasetaite, S. Rekštytė, V. Raudoniene, D. Bridziuviene, M. Malinauskas and J. Ostrauskaite, Vanillin Acrylate-Based Resins for Optical 3D Printing, *Polymers (Basel).*, 2020, **12**, 397.

24 C. H. Zhao, R. K. Zhang, B. Qiao, B. Z. Li and Y. J. Yuan, Engineering budding yeast for the production of coumarins from lignin, *Biochem. Eng. J.*, 2020, **160**, 107634.

25 T. Matsuda, M. Mizutani and S. C. Arnold, Molecular design of photocurable liquid biodegradable copolymers. 1. Synthesis and photocuring characteristics, *Macromolecules*, 2000, **33**, 795–800.

26 W. Guerin, M. Helou, M. Slawinski, J. M. Brusson, J. F. Carpentier and S. M. Guillaume, Macromolecular engineering via ring-opening polymerization (3): Trimethylene carbonate block copolymers derived from glycerol, *Polym. Chem.*, 2014, **5**, 1229–1240.

27 Z. Zhang, J. Song and B. Han, Catalytic Transformation of Lignocellulose into Chemicals and Fuel Products in Ionic Liquids, *Chem. Rev.*, 2017, **117**, 6834–6880.

28 A. J. D. Silvestre and A. Gandini, in *Monomers, Polymers and Composites from Renewable Resources*, eds. M. Naceur Belgacem and A. Gandini, Elsevier, 2008, pp. 67–88.

29 C. Lu, C. Wang, J. Yu, J. Wang and F. Chu, Two-Step 3 D-Printing Approach toward Sustainable, Repairable, Fluorescent Shape-Memory Thermosets Derived from Cellulose and Rosin, *ChemSusChem*, 2019, **210037**, 1–11.

30 S. D. Silbert, P. Simpson, R. Setien, M. Holthaus, J. La Scala, C. A. Ulven and D. C. Webster, Exploration of Bio-Based Functionalized Sucrose Ester Resins for Additive Manufacturing via Stereolithography, *ACS Appl. Polym. Mater.*, 2020, **2**, 2910–2918.

31 L. Elomaa, S. Teixeira, R. Hakala, H. Korhonen, D. W. Grijpma and J. V. Seppälä, Preparation of poly(ε-caprolactone)-based tissue engineering scaffolds by stereolithography, *Acta Biomater.*, 2011, **7**, 3850–3856.

32 M. Zarek, M. Layani, I. Cooperstein, E. Sachyani, D. Cohn and S. Magdassi, 3D Printing of Shape Memory Polymers for Flexible Electronic Devices, *Adv. Mater.*, 2016, **28**, 4449–4454.

33 T. Kuhnt, R. Marroquín García, S. Camarero-Espinosa, A. Dias, A. T. Ten Cate, C. A. Van Blitterswijk, L. Moroni and M. B. Baker, Poly(caprolactone -co -trimethylenecarbonate) urethane acrylate resins for digital light processing of bioresorbable tissue engineering implants, *Biomater. Sci.*, 2019, **7**, 4984–4989.

34 L. Elomaa, Y. Kang, J. V. Seppälä and Y. Yang, Biodegradable photocrosslinkable poly(depsipeptide- co -ε-caprolactone) for tissue engineering: Synthesis, characterization, and In vitro evaluation, *J. Polym. Sci. Part A Polym. Chem.*, 2014, **52**, 3307–3315.

35 J.-Y. Chen, J. Hwang, W.-S. Ao-Ieong, Y.-C. Lin, Y.-K. Hsieh, Y.-L. Cheng and J. Wang, Study of Physical and Degradation Properties of 3D-Printed Biodegradable, Photocurable Copolymers, PGSA-co-PEGDA and PGSA-co-PCLDA, *Polymers (Basel).*, 2018, **10**, 1263.

36 A. R. Johnson, C. L. Caudill, J. R. Tumbleston, C. J. Bloomquist, K. A. Moga, A. Ermoshkin, D. Shirvanyants, S. J. Mecham, J. C. Luft and J. M. DeSimone, Single-Step Fabrication of Computationally Designed Microneedles by Continuous Liquid Interface Production, *PLoS One*, 2016, **11**, e0162518.

37 F. P. W. Melchels, J. Feijen and D. W. Grijpma, A poly(d,l-lactide) resin for the preparation of tissue engineering scaffolds by stereolithography, *Biomaterials*, 2009, **30**, 3801–3809.

38 J. Jansen, F. P. W. Melchels, D. W. Grijpma and J. Feijen, Fumaric acid monoethyl ester-functionalized poly(D,L-Lactide)/N-vinyl-2- pyrrolidone Resins for the preparation of tissue engineering scaffolds by stereolithography, *Biomacromolecules*, 2009, **10**, 214–220.

39 R. M. Felfel, L. Poocza, M. Gimeno-Fabra, T. Milde, G. Hildebrand, I. Ahmed, C. Scotchford, V. Sottile, D. M. Grant and K. Liefeith, In vitro degradation and mechanical properties of PLA-PCL copolymer unit cell scaffolds generated by two-photon polymerization, *Biomed. Mater.*, 2016, **11**, 015011.

40 T. Werpy and G. Petersen, *Top Value Added Chemicals from Biomass: Volume I -- Results of Screening for Potential Candidates from Sugars and Synthesis Gas*, Golden, CO (United States), 2004.

41 R. Mülhaupt, Green Polymer Chemistry and Bio-based Plastics: Dreams and Reality, *Macromol. Chem. Phys.*, 2013, **214**, 159–174.

42 X. Zhuang, O. Kilian, E. Monroe, M. Ito, M. B. Tran-Gymfi, F. Liu, R. W. Davis, M. Mirsiaghi, E. Sundstrom, T. Pray, J. M. Skerker, A. George and J. M. Gladden, Monoterpene production by the carotenogenic yeast Rhodosporidium toruloides, *Microb. Cell Fact.*, 2019, **18**, 1–15.

43 A. C. Weems, K. R. Delle Chiaie, J. C. Worch, C. J. Stubbs and A. P. Dove, Terpene- and terpenoid-based polymeric resins for stereolithography 3D printing, *Polym. Chem.*, 2019, **10**, 5959–5966.

44 A. C. Weems, K. R. Delle Chiaie, R. Yee and A. P. Dove, Selective Reactivity of Myrcene for Vat Photopolymerization 3D Printing and Postfabrication Surface Modification, *Biomacromolecules*, 2020, **21**, 163–170.

45 F. A. M. M. Gonçalves, C. S. M. F. Costa, I. G. P. Fabela, D. Farinha, H. Faneca, P. N. Simões, A. C. Serra, P. J. Bártolo and J. F. J. Coelho, 3D printing of new biobased unsaturated polyesters by microstereo-thermal-lithography, *Biofabrication*, 2014, **6**, 035024.

46 J.-T. Miao, S. Peng, M. Ge, Y. Li, J. Zhong, Z. Weng, L. Wu and L. Zheng, Three-Dimensional Printing Fully Biobased Heat-Resistant Photoactive Acrylates from Aliphatic Biomass, *ACS Sustain. Chem. Eng.*, 2020, **8**, 9415–9424.

47 B. George, A. Caldwell, T. Lee and M. Snyder, Global Corn Oil Trade Falls with Increased Competition and Tighter U.S. Supplies, July 2020, https://apps.fas.usda.gov/psdonline/app/index.html#/app/downloads, (accessed 15 July 2020).

48 A. Bayrak, M. Kiralan, A. Ipek, N. Arslan, B. Cosge and K. M. Khawar, Fatty acid compositions of linseed (Linum Usitatissimum L.) genotypes of different origin cultivated

in Turkey, *Biotechnol. Biotechnol. Equip.*, 2010, **24**, 1836–1842.

49 T. E. Clemente and E. B. Cahoon, Soybean oil: Genetic approaches for modification of functionality and total content, *Plant Physiol.*, 2009, **151**, 1030–1040.

50 E. Skliutas, S. Kašėtaitė, G. Grigalevičiūtė, L. Jonušauskas, S. Rekštytė, J. Ostrauskaitė and M. Malinauskas, in *Advanced Fabrication Technologies for Micro/Nano Optics and Photonics X*, eds. G. von Freymann, W. V. Schoenfeld and R. C. Rumpf, 2017, vol. 10115, p. 1011514.

51 E. Skliutas, S. Kasetaite, L. Jonušauskas, J. Ostrauskaite and M. Malinauskas, Photosensitive naturally derived resins toward optical 3-D printing, *Opt. Eng.*, 2018, **57**, 1.

52 A. Bagheri and J. Jin, Photopolymerization in 3D Printing, *ACS Appl. Polym. Mater.*, 2019, **1**, 593–611.

53 E. Skliutas, M. Lebedevaite, S. Kasetaite, S. Rekštytė, S. Lileikis, J. Ostrauskaite and M. Malinauskas, A Bio-Based Resin for a Multi-Scale Optical 3D Printing, *Sci. Rep.*, 2020, **10**, 9758.

54 M. Lebedevaite, J. Ostrauskaite, E. Skliutas and M. Malinauskas, Photoinitiator Free Resins Composed of Plant-Derived Monomers for the Optical μ-3D Printing of Thermosets, *Polymers (Basel).*, 2019, **11**, 116.

55 J. Guit, M. B. L. Tavares, J. Hul, C. Ye, K. Loos, J. Jager, R. Folkersma and V. S. D. Voet, Photopolymer Resins with Biobased Methacrylates Based on Soybean Oil for Stereolithography, *ACS Appl. Polym. Mater.*, 2020, **2**, 949–957.

56 S. Miao, W. Zhu, N. J. Castro, M. Nowicki, X. Zhou, H. Cui, J. P. Fisher and L. G. Zhang, 4D printing smart biomedical scaffolds with novel soybean oil epoxidized acrylate, *Sci. Rep.*, 2016, **6**, 27226.

57 A. Halász, Á. Baráth, L. Simon-Sarkadi and W. Holzapfel, Biogenic amines and their production by microorganisms in food, *Trends Food Sci. Technol.*, 1994, **5**, 42–49.

58 R. L. Whistler, *Industrial gums, polysaccharides and their derivatives*, Academic Press, New York, 1959.

59 A. LINKER and R. S. JONES, A Polysaccharide resembling Alginic Acid from a Pseudomonas Micro-organism, *Nature*, 1964, **204**, 187–188.

60 J. R. W. GOVAN, J. A. M. FYFE and T. R. JARMAN, Isolation of Alginate-producing Mutants of Pseudomonas fluorescens, Pseudomonas putida and Pseudomonas mendocina, *Microbiology*, 1981, **125**, 217–220.

61 J. H. Sze, J. C. Brownlie and C. A. Love, Biotechnological production of hyaluronic acid: a mini review, *3 Biotech*, 2016, **6**, 67.

62 H. Hong, Y. B. Seo, D. Y. Kim, J. S. Lee, Y. J. Lee, H. Lee, O. Ajiteru, M. T. Sultan, O. J. Lee, S. H. Kim and C. H. Park, Digital light processing 3D printed silk fibroin hydrogel for cartilage tissue engineering, *Biomaterials*, 2020, **232**, 119679.

63 R. Raoufinia, A. Mota, N. Keyhanvar, F. Safari, S. Shamekhi and J. Abdolalizadeh, Overview of Albumin and Its Purification Methods, *Adv. Pharm. Bull.*, 2016, **6**, 495–507.

64 G. N. Ramachandran, *Treatise on collagen*, Academic Press, London, New York, 1967, vol. 1.

65 J. Van Hoorick, L. Tytgat, A. Dobos, H. Ottevaere, J. Van Erps, H. Thienpont, A. Ovsianikov, P. Dubruel and S. Van Vlierberghe, (Photo-)crosslinkable gelatin derivatives for biofabrication applications, *Acta Biomater.*, 2019, **97**, 46–73.

66 S. H. Pyo, P. Wang, H. H. Hwang, W. Zhu, J. Warner and S. Chen, Continuous optical 3D printing of green aliphatic polyurethanes, *ACS Appl. Mater. Interfaces*, 2017, **9**, 836–844.

67 J. J. Warner, P. Wang, W. M. Mellor, H. H. Hwang, J. H. Park, S. H. Pyo and S. Chen, 3D printable non-isocyanate polyurethanes with tunable material properties, *Polym. Chem.*, 2019, **10**, 4665–4674.

68 S. H. Pyo and R. Hatti-Kaul, Chlorine-Free Synthesis of Organic Alkyl Carbonates and Five- and Six-Membered Cyclic Carbonates, *Adv. Synth. Catal.*, 2016, **358**, 834–839.

69 Y.-C. Chiu, Y.-F. Shen, A. K.-X. Lee, S.-H. Lin, Y.-C. Wu and Y.-W. Chen, 3D Printing of Amino Resin-based Photosensitive Materials on Multi-parameter Optimization Design for Vascular Engineering Applications, *Polymers (Basel).*, 2019, **11**, 1394.

70 US 8,362,148, 2013.

71 P. T. Smith, B. Narupai, J. H. Tsui, S. C. Millik, R. T. Shafranek, D.-H. Kim and A. Nelson, Additive Manufacturing of Bovine Serum Albumin-Based Hydrogels and Bioplastics, *Biomacromolecules*, 2020, **21**, 484–492.

72 M.-Y. Shie, W.-C. Chang, L.-J. Wei, Y.-H. Huang, C.-H. Chen, C.-T. Shih, Y.-W. Chen and Y.-F. Shen, 3D Printing of Cytocompatible Water-Based Light-Cured Polyurethane with Hyaluronic Acid for Cartilage Tissue Engineering Applications, *Materials (Basel).*, 2017, **10**, 136.

73 T. M. Valentin, S. E. Leggett, P.-Y. Chen, J. K. Sodhi, L. H. Stephens, H. D. McClintock, J. Y. Sim and I. Y. Wong, Stereolithographic printing of ionically-crosslinked alginate hydrogels for degradable biomaterials and microfluidics, *Lab Chip*, 2017, **17**, 3474–3488.

74 J. K. Placone, J. Navarro, G. W. Laslo, M. J. Lerman, A. R. Gabard, G. J. Herendeen, E. E. Falco, S. Tomblyn, L. Burnett and J. P. Fisher, Development and Characterization of a 3D Printed, Keratin-Based Hydrogel, *Ann. Biomed. Eng.*, 2017, **45**, 237–248.

75 B. Wu, A. Sufi, R. Ghosh Biswas, A. Hisatsune, V. Moxley-Paquette, P. Ning, R. Soong,

A. P. Dicks and A. J. Simpson, Direct Conversion of McDonald's Waste Cooking Oil into a Biodegradable High-Resolution 3D-Printing Resin, *ACS Sustain. Chem. Eng.*, 2020, **8**, 1171–1177.

76 V. Schimpf, A. Asmacher, A. Fuchs, B. Bruchmann and R. Mülhaupt, Polyfunctional Acrylic Non-isocyanate Hydroxyurethanes as Photocurable Thermosets for 3D Printing, *Macromolecules*, 2019, **52**, 3288–3297.

77 M. D. Alim, K. K. Childress, N. J. Baugh, A. M. Martinez, A. Davenport, B. D. Fairbanks, M. K. McBride, B. T. Worrell, J. W. Stansbury, R. R. McLeod and C. N. Bowman, A photopolymerizable thermoplastic with tunable mechanical performance, *Mater. Horizons*, 2020, **7**, 835–842.

78 S. Deng, J. Wu, M. D. Dickey, Q. Zhao and T. Xie, Rapid Open-Air Digital Light 3D Printing of Thermoplastic Polymer, *Adv. Mater.*, 2019, **31**, 1903970.

79 A. Li, A. Challapalli and G. Li, 4D Printing of Recyclable Lightweight Architectures Using High Recovery Stress Shape Memory Polymer, *Sci. Rep.*, 2019, **9**, 7621.

80 B. Zhang, K. Kowsari, A. Serjouei, M. L. Dunn and Q. Ge, Reprocessable thermosets for sustainable three-dimensional printing, *Nat. Commun.*, 2018, **9**, 1831.

81 X. Li, R. Yu, Y. He, Y. Zhang, X. Yang, X. Zhao and W. Huang, Four-dimensional printing of shape memory polyurethanes with high strength and recyclability based on Diels-Alder chemistry, *Polymer (Guildf).*, 2020, **200**, 122532.

82 S. Ma and D. C. Webster, Degradable thermosets based on labile bonds or linkages: A review, *Prog. Polym. Sci.*, 2018, **76**, 65–110.

83 B. Laycock, M. Nikolić, J. M. Colwell, E. Gauthier, P. Halley, S. Bottle and G. George, Lifetime prediction of biodegradable polymers, *Prog. Polym. Sci.*, 2017, **71**, 144–189.

84 T. M. Seck, F. P. W. Melchels, J. Feijen and D. W. Grijpma, Designed biodegradable hydrogel structures prepared by stereolithography using poly(ethylene glycol)/poly(d,l-lactide)-based resins, *J. Control. Release*, 2010, **148**, 34–41.

85 S. Sharifi, S. B. G. Blanquer, T. G. Van Kooten and D. W. Grijpma, Biodegradable nanocomposite hydrogel structures with enhanced mechanical properties prepared by photo-crosslinking solutions of poly(trimethylene carbonate)-poly(ethylene glycol)-poly(trimethylene carbonate) macromonomers and nanoclay particles, *Acta Biomater.*, 2012, **8**, 4233–4243.

86 J. M. Walker, E. Bodamer, O. Krebs, Y. Luo, A. Kleinfehn, M. L. Becker and D. Dean, Effect of Chemical and Physical Properties on the In Vitro Degradation of 3D Printed High Resolution Poly(propylene fumarate) Scaffolds, *Biomacromolecules*, 2017, **18**, 1419–1425.

87 Y. Luo, C. K. Dolder, J. M. Walker, R. Mishra, D. Dean and M. L. Becker, Synthesis and Biological Evaluation of Well-Defined Poly(propylene fumarate) Oligomers and Their Use

in 3D Printed Scaffolds, *Biomacromolecules*, 2016, **17**, 690–697.

88 J. M. Sirrine, A. M. Pekkanen, A. M. Nelson, N. A. Chartrain, C. B. Williams and T. E. Long, 3D-Printable Biodegradable Polyester Tissue Scaffolds for Cell Adhesion, *Aust. J. Chem.*, 2015, **68**, 1409–1414.

89 A. Oesterreicher, J. Wiener, M. Roth, A. Moser, R. Gmeiner, M. Edler, G. Pinter and T. Griesser, Tough and degradable photopolymers derived from alkyne monomers for 3D printing of biomedical materials, *Polym. Chem.*, 2016, **7**, 5169–5180.

90 X. Wang, X. H. Qin, C. Hu, A. Terzopoulou, X. Z. Chen, T. Y. Huang, K. Maniura-Weber, S. Pané and B. J. Nelson, 3D Printed Enzymatically Biodegradable Soft Helical Microswimmers, *Adv. Funct. Mater.*, 2018, **28**, 1–8.

91 C. Wang, T. M. Goldman, B. T. Worrell, M. K. McBride, M. D. Alim and C. N. Bowman, Recyclable and repolymerizable thiol–X photopolymers, *Mater. Horizons*, 2018, **5**, 1042–1046.

92 D. E. Fagnani, J. L. Tami, G. Copley, M. N. Clemons, Y. D. Y. L. Getzler and A. J. McNeil, 100th Anniversary of Macromolecular Science Viewpoint: Redefining Sustainable Polymers, *ACS Macro Lett.*, 2021, **10**, 41–53.

93 X. Li, R. Yu, Y. He, Y. Zhang, X. Yang, X. Zhao and W. Huang, Self-Healing Polyurethane Elastomers Based on a Disulfide Bond by Digital Light Processing 3D Printing, *ACS Macro Lett.*, 2019, **8**, 1511–1516.